Article:
Inskip, K.J., Best, P.N. and Longair, M.S. (2006) Deviations from passive evolution – star formation and the ultraviolet excess in z ∼ 1 radio galaxies. Monthly Notices of the Royal Astronomical Society, 367 (2). pp. 693-708. ISSN 0035-8711

https://doi.org/10.1111/j.1365-2966.2006.10005.x

Mon. Not. R. Astron. Soc. **367,** 693–708 (2006) doi:10.1111/j.1365-2966.2006.10005.x

Deviations from passive evolution – star formation and the ultraviolet excess in $z \sim 1$ radio galaxies

K. J. Inskip,[1,2]★ P. N. Best[3] and M. S. Longair[2]

[1]*Department of Physics & Astronomy, University of Sheffield, Sheffield S3 7RH*
[2]*Cavendish Laboratory, Madingley Road, Cambridge, CB3 0HE*
[3]*Institute for Astronomy, Royal Observatory Edinburgh, Blackford Hill, Edinburgh, EH9 3HJ*

Accepted 2005 December 7. Received 2005 December 2; in original form 2005 June 30

ABSTRACT

Galaxy colours are determined for two samples of 6C and 3CR radio sources at $z \sim 1$, differing by a factor of ∼6 in radio power. Corrections are made for emission-line contamination and the presence of any nuclear point source, and the data analysed as a function of both redshift and the radio source properties. The galaxy colours are remarkably similar for the two populations, and the ultraviolet excess evolves with radio source size similarly in both samples, despite the fact that the alignment effect is more extensive for the more powerful 3CR radio galaxies. These results seem to suggest that the alignment effect at these redshifts does not scale strongly with radio power, and is instead more closely dependent on galaxy mass (which is statistically comparable for the two samples). However, it is likely that the presence of relatively young ($\lesssim$several times 10^8-yr-old) stellar populations has considerably contaminated the K-band flux of these systems, particularly in the case of the more powerful 3CR sources, which are ∼0.5 mag more luminous than the predictions of passive evolution models at $z \sim 1$. The higher luminosity of the 3CR alignment effect is balanced by emission at longer wavelengths, thereby leading to comparable colours for the two samples.

Key words: galaxies: active – galaxies: evolution – galaxies: photometry.

1 INTRODUCTION

The properties of powerful radio sources vary considerably with both radio power and redshift. Up to redshifts of $z \sim 1$, radio sources are usually hosted by massive elliptical galaxies, with scale sizes of ∼10–15 kpc (e.g. McLure et al. 2004; Inskip et al. 2005). Whilst the average galaxy size does not appear to vary greatly, the host galaxies of the higher redshift radio sources within this redshift range ($z \gtrsim 0.6$) are intrinsically more luminous than those at lower redshifts (Inskip et al. 2002a, 2005), to an extent which implies that factors other than simple passive evolution are involved. At larger redshifts ($z > 2$), the host galaxies of the most distant radio sources are clearly still in the process of formation (e.g. van Breugel et al. 1998; Pentericci et al. 2001).

Redshift evolution is also observed in the emission surrounding the host galaxies. At $z > 0.3$, the host galaxies are often seen to be surrounded by considerable excess rest-frame ultraviolet (UV) emission; at higher redshifts ($z \gtrsim 0.6$) this emission is usually more extensive, is generally observed to be closely aligned with the radio source axis (Chambers, Miley & van Breugel 1987; McCarthy et al. 1987; Allen et al. 2002), and is known as the *alignment effect*. Both the alignment effect and the properties of the extended emission-line regions surrounding these sources are seen to be more extreme (in terms of luminosity, alignment with the radio axis, physical extent and gas kinematics) both for more powerful radio sources, and also for the smaller radio sources (Best, Longair & Röttgering 1996; Best, Röttgering & Longair 2000b; Inskip et al. 2002c, 2003, 2005). Several different mechanisms are thought to be responsible for producing these regions of extensive aligned emission. These include extended line emission and nebular continuum radiation (Dickson et al. 1995), scattering of the UV continuum from the active galactic nucleus/nuclei (AGN) (e.g. Tadhunter et al. 1992; Cimatti et al. 1993) and young stars (e.g. Chambers & McCarthy 1990) potentially produced in a radio jet induced starburst (McCarthy et al. 1987). Merger-induced starbursts may also be responsible for the presence of a relatively young stellar population in/around the host galaxy (Tadhunter et al. 2005, and references therein).

McCarthy, Spinrad & van Breugel (1995) found that extended line emission can be observed around the majority of 3CR galaxies at $z \gtrsim 0.3$. The relative contribution of emission lines to the total aligned emission varies from source to source, although both the alignment effect and emission-line flux are more extreme for smaller radio sources. Typically, line emission provides from 2 to 30 per cent of the total rest-frame UV aligned emission for 3CR galaxies at $z \sim 1$ (although this does depend on the distribution of emission

★E-mail: k.inskip@shef.ac.uk

lines within the wavelength range of the observed filter), with similar proportions found for the less powerful 6C radio sources at the same redshifts (Best 1996; Inskip et al. 2003). In addition to line emission, nebular continuum radiation is also produced due to other radiative processes associated with the ionized gas. Although a significant process for some sources, the total flux provided by line emission and nebular continuum emission alone cannot account for all of the excess emission forming the alignment effect (e.g. Tadhunter et al. 2002; Inskip et al. 2003).

Although the active nucleus of a radio galaxy may be obscured from view, the powerful UV continuum emitted by the AGN may be scattered towards an observer by dust or electrons in the extended structures surrounding the galaxy. Emission polarized perpendicularly to the direction of emission from the AGN due to scattering has been observed from these extended regions, and is consistent with the orientation-based unification scheme for radio galaxies and quasars (e.g. Cimatti et al. 1993; Tran et al. 1998). However, while polarized emission is frequently observed, the emission from the aligned structures surrounding many radio galaxies lacks the high levels of polarization expected if scattering of the UV emission from the obscured quasar nucleus were the only mechanism occurring. A recent study of $0.15 < z < 0.7$ radio galaxies by Tadhunter et al. (2002) found that scattering contributed a significant proportion of the UV excess in many cases, but was very rarely the dominant factor. Further to this, some 3CR sources do not exhibit any polarization of their extended structures (e.g. Wills et al. 2002).

Finally, one of the first explanations proposed for the excess UV continuum was that it was due to emission from young stars, whose formation was triggered by the passage of the expanding radio source (e.g. Chambers et al. 1987; McCarthy et al. 1987). The emission from such a population of hot, young stars would dominate the UV emission of the galaxy, and produce a fairly flat spectral shape, whilst at near infrared wavelengths, the emission would still be predominantly due to the old stellar population of the host galaxy. Any young stellar population (YSP) would quickly (within $\lesssim 10^7$ yr) evolve, accounting for the rapid evolution with radio size seen in the UV aligned structures at $z \sim 1$ (Best et al. 1996). In order to account for the excess emission, the mass of stars formed in the interactions with the radio source is typically required to be only a few times $10^8\,\mathrm{M}_\odot$(e.g. Best, Longair & Röttgering 1997a). It is questionable how easily jet-induced star formation can occur. Numerical simulations in the literature often disagree on whether clouds will be compressed or shredded/dissipated (e.g. Begelman & Cioffi 1989; Rees 1989; Klein, McKee & Colella 1994; Icke 1999; Poludnenko, Frank & Blackman 2002), although recent work including the effects of cooling (e.g. Mellema, Kurk & Röttgering 2002) suggests that such triggered star formation is indeed plausible. Observational evidence for star formation triggered by the radio source jets is seen in isolated objects: 3C 34 (Best et al. 1997a), Minkowski's object (van Breugel et al. 1985), 3C 285 (van Breugel & Dey 1993).

Evidence that shocks strongly influence the ionization and kinematics of the emission-line gas has been observed in the spectra of many distant radio sources (e.g. Best, Röttgering & Longair 2000b; Solórzano-Iñarrea, Tadhunter & Axon 2001; Inskip et al. 2002b), particularly in the case of smaller radio sources, i.e. those with a projected physical size of $<$120 kpc. We also find that the sources in which shocks have the greatest impact on the emission-line gas properties are those with the most extensive, luminous alignment effects (Inskip et al. 2002c, 2005). The shocks associated with an expanding radio source can greatly influence the alignment effect. Ionizing photons associated with the shocks may boost certain emission lines, and also lead to an increase in nebular continuum emission. Star formation induced by the passage of radio source shocks through the cool dense gas clouds is also an obvious mechanism by which the alignment effect may be enhanced. In addition, the passage of a fast shock can potentially cause the breakup of optically thick clouds (Bremer, Fabian & Crawford 1997), increasing the covering factor for scattering of the UV flux from the AGN. The more numerous, smaller clouds will also have a larger cross-section for ionization by the AGN, leading to an increase in the total flux of line emission.

Despite the compelling evidence for each of the alignment effect mechanisms outlined above, their relative balance is still poorly understood. A wide range of galaxy colours provides a useful means of probing the contributions from different physical processes, and their dependence on the properties of the radio source population (power, size, epoch). This is of particular interest, since the dependence of different mechanisms on each of these parameters varies significantly. For example, line emission is known to be closely linked to both radio source power and size. Star formation, on the other hand, may be independent of radio power, despite evolving quickly with age. It is necessary that these processes are better understood before we can interpret the clear redshift evolution of the alignment effect.

One problem with studies of 3CR radio galaxies is that the radio power of sources in a flux-limited sample such as this increases with redshift, leading to a degeneracy between redshift and radio power. The less powerful 6C sample provides a population of radio galaxies ideally suited for breaking this degeneracy. The factor of $\sim$6 difference in radio power between the samples is small compared to the wide range of powers (spanning several orders of magnitude) observed for the radio source population as a whole. However, it is comparable to the difference in power between 3C sources at low ($z \sim 0.1$–0.5) and high ($z \sim 1$) redshifts, and it is the evolution within this range that we hope to explain. To this end, we have carried out a program of multiwavelength imaging and spectroscopic observations of a subsample of 11 6C radio sources at $z \sim 1$ (Best et al. 1999; Inskip et al. 2002b, 2003), which are well matched to the 3CR subsample previously studied by Best et al. (1997b) and Best, Röttgering & Longair (2000a). Having already analysed the spectroscopic (Inskip et al. 2002c) and morphological properties of these systems (Inskip et al. 2005, which included an analysis of the variations in host galaxy size), we now turn our attention to investigating the effect of radio power on the galaxy colours, and the nature of the excess UV emission (including the relative contributions of line emission and nebular continuum). The structure of the paper is as follows. In Section 2, we briefly outline the sample selection and observations. Colours are determined for the two matched samples, including emission-line corrections. The results are presented in Section 3, and analysed in more depth in Section 4, where we consider the influence of radio source size and power. We consider the influence of the host galaxy stellar populations in Section 5, and present our conclusions in Section 6. Values for the cosmological parameters $\Omega_0 = 0.3, \Omega_\Lambda = 0.7$ and $H_0 = 65\,\mathrm{km\,s^{-1}\,Mpc^{-1}}$ are assumed throughout this paper.

2 GALAXY COLOURS FOR 3CR AND 6C RADIO SOURCES

2.1 Sample selection and observations

This paper focuses on observations of galaxies selected from two well-matched radio galaxy subsamples at $z \sim 1$, which have been

extensively studied using the *Hubble Space Telescope* (*HST*), the Very Large Array and the United Kingdom Infrared Telescope (UKIRT). The 3CR subsample consists of 28 galaxies with $0.6 < z < 1.8$ (see Best, Longair & Röttgering 1997b, 1998, for a description of the sample and the imaging observations and results). The 6C comparison sample consists of 11 radio galaxies at $0.85 < z < 1.5$, which are approximately six times less powerful radio sources than 3CR sources at the same redshift. Full selection criteria and details of the observations of these 6C sources can be found in Papers I and II of this series (Inskip et al. 2003, 2005) and also Best et al. (1999). Deep spectroscopic observations are also available for a subset of 14 3CR galaxies with $0.7 < z < 1.25$ and the eight 6C sources with $0.85 < z < 1.3$ (Best et al. 2000a,b; Inskip et al. 2002b).

2.2 Calculating the colours

The *HST*/Wide Field Planetary Camera 2 (WFPC2) and UKIRT magnitudes previously presented for the 3CR and 6C sources (Best et al. 1997b; Inskip et al. 2003) were determined through 9 arcsec diameter apertures. The advantage of this approach was that such an aperture includes essentially all the light emitted from the galaxy. However, for several sources the 9 arcsec diameter apertures are contaminated by flux from other nearby objects. For the current analysis, we use galaxy magnitudes determined within a 4 arcsec diameter aperture (see Table 1), where removal of flux from nearby companion objects is not usually required. The exception to this rule is an unresolved point source in close proximity to the host galaxy

Table 1. Observed (roman) and calculated (italics) magnitudes for the 6C and 3CR sources at $z \sim 1$, together with a summary of the source redshifts, radio sizes and radio power at 178 MHz. All magnitudes for the sources in both samples were determined within a 4 arcsec diameter aperture and have been corrected for galactic extinction. The 6C data were previously presented in Inskip et al. (2003). The 3CR *HST*, *J*- and *K*-band data were initially analysed in 5- and 9-arcsec apertures (Best et al. 1997), but magnitudes have been re-extracted in 4 arcsec diameter apertures for the purposes of this paper. The *H*-band 3CR data were obtained via the UKIRT service program. For 6C 1256+36, the flux due to the unresolved companion object has been modelled (Inskip et al. 2005, Paper II) and removed from the F702W and *K*-band data (magnitudes which remain contaminated by this object are marked by a '*'). No corrections have been made for flux contamination in the *HST* data by adjacent objects, as it is usually impossible to disentangle adjacent galaxies from any aligned line/continuum emission.

Source	Redshift	L_{178} ($\log_{10}$ W Hz^{-1})	$D_{\rm rad}$ (kpc)	F702W	F814W	*J*	*H*	*K*
6C 0825+34	1.467	28.31	64	*22.59 ± 0.31*	22.10 ± 0.17	19.86 ± 0.17	19.68 ± 0.29	19.12 ± 0.12
6C 0943+39	1.035	28.07	92	22.08 ± 0.14	*21.55 ± 0.20*	19.70 ± 0.12	19.27 ± 0.14	18.09 ± 0.07
6C 1011+36	1.042	28.02	444	21.73 ± 0.07	*21.23 ± 0.15*	19.68 ± 0.20	18.63 ± 0.10	17.83 ± 0.06
6C 1017+37	1.053	28.10	65	21.77 ± 0.06	*21.10 ± 0.14*	19.89 ± 0.16	19.54 ± 0.15	18.57 ± 0.09
6C 1019+39	0.922	28.03	67	*21.04 ± 0.29*	20.07 ± 0.04	18.47 ± 0.07	17.71 ± 0.06	16.80 ± 0.04
6C 1100+35	1.440	28.32	119	*22.31 ± 0.26*	21.80 ± 0.06	19.59 ± 0.12	19.02 ± 0.11	17.99 ± 0.07
6C 1129+37	1.060	28.03	141	22.02 ± 0.07	*21.64 ± 0.16*	19.35 ± 0.11	18.31 ± 0.09	17.81 ± 0.07
6C 1204+35	1.376	28.45	158	*21.84 ± 0.28*	21.30 ± 0.10	19.31 ± 0.11	18.76 ± 0.11	18.01 ± 0.07
6C 1217+36	1.088	28.12	38	*21.91 ± 0.25*	20.89 ± 0.05	19.50 ± 0.12	18.51 ± 0.07	17.55 ± 0.06
6C 1256+36	1.128	28.20	155	22.86 ± 0.09	*22.60 ± 0.16**	19.74 ± 0.20*	18.58 ± 0.09*	18.14 ± 0.06
6C 1257+36	1.004	28.06	336	*21.55 ± 0.30*	20.98 ± 0.05	19.39 ± 0.11	18.27 ± 0.07	17.50 ± 0.05
3C 13	1.351	29.20	259	*21.16 ± 0.25*	20.57 ± 0.03	18.74 ± 0.13	–	17.47 ± 0.11
3C 22	0.938	28.77	209	*20.00 ± 0.15*	19.29 ± 0.02	17.53 ± 0.08	16.95 ± 0.09	15.66 ± 0.05
3C 34	0.690	28.51	359	*20.70 ± 0.25*	*20.03 ± 0.25*	18.30 ± 0.11	–	16.46 ± 0.07
3C 41	0.795	28.48	194	*20.42 ± 0.20*	*19.79 ± 0.20*	18.78 ± 0.14	–	15.89 ± 0.05
3C 49	0.621	28.25	7	*19.97 ± 0.15*	19.33 ± 0.05	–	–	16.25 ± 0.06
3C 65	1.176	29.09	160	*22.08 ± 0.16*	21.07 ± 0.03	18.93 ± 0.14	–	17.19 ± 0.10
3C 68.2	1.575	29.33	218	*22.37 ± 0.30*	*21.87 ± 0.30*	19.78 ± 0.22	–	18.18 ± 0.16
3C 217	0.897	28.69	110	*20.81 ± 0.17*	20.27 ± 0.02	18.81 ± 0.13	18.99 ± 0.23	17.88 ± 0.13
3C 226	0.820	28.75	259	*20.46 ± 0.18*	*19.64 ± 0.16*	18.46 ± 0.11	17.82 ± 0.13	16.83 ± 0.08
3C 239	1.781	29.60	111	*21.60 ± 0.20*	21.16 ± 0.03	19.01 ± 0.14	–	17.90 ± 0.13
3C 241	1.617	29.39	8	*22.19 ± 0.20*	21.62 ± 0.04	19.19 ± 0.16	–	17.82 ± 0.13
3C 247	0.749	28.44	110	*20.35 ± 0.24*	19.46 ± 0.02	–	–	16.04 ± 0.06
3C 252	1.105	28.98	501	*21.10 ± 0.13*	20.58 ± 0.03	–	–	17.54 ± 0.11
3C 265	0.811	28.88	636	*19.51 ± 0.24*	*19.06 ± 0.30*	17.81 ± 0.08	17.52 ± 0.11	16.39 ± 0.07
3C 266	1.272	29.13	41	21.22 ± 0.03	20.55 ± 0.03	–	–	17.99 ± 0.14
3C 267	1.144	29.11	339	21.50 ± 0.04	*20.95 ± 0.10*	19.20 ± 0.16	–	17.46 ± 0.11
3C 277.2	0.766	28.62	422	*20.16 ± 0.20*	19.82 ± 0.02	18.59 ± 0.12	–	17.32 ± 0.10
3C 280	0.996	29.13	118	*20.92 ± 0.06*	20.29 ± 0.02	18.48 ± 0.11	18.10 ± 0.15	17.05 ± 0.09
3C 289	0.967	28.81	90	*21.49 ± 0.07*	20.50 ± 0.03	18.66 ± 0.12	17.97 ± 0.14	17.06 ± 0.09
3C 324	1.206	29.18	100	21.49 ± 0.03	*20.84 ± 0.20*	19.18 ± 0.17	18.30 ± 0.16	17.33 ± 0.10
3C 337	0.635	28.32	326	*20.79 ± 0.25*	19.94 ± 0.02	18.45 ± 0.11	–	16.84 ± 0.08
3C 340	0.775	28.48	363	*20.88 ± 0.18*	*19.71 ± 0.21*	18.52 ± 0.12	17.89 ± 0.12	17.08 ± 0.09
3C 352	0.806	28.61	100	*20.63 ± 0.08*	20.14 ± 0.02	–	–	17.09 ± 0.09
3C 356	1.079	28.96	638	*21.22 ± 0.09*	20.60 ± 0.03	–	–	17.54 ± 0.11
3C 368	1.132	29.17	75	20.47 ± 0.02	*19.55 ± 0.08*	19.01 ± 0.11	17.83 ± 0.13	17.17 ± 0.10
3C 437	1.480	29.32	339	*22.38 ± 0.30*	*21.86 ± 0.30*	–	–	18.23 ± 0.16
3C 441	0.708	28.51	257	*20.07 ± 0.15*	*19.28 ± 0.15*	18.15 ± 0.10	–	16.49 ± 0.07
3C 470	1.653	29.20	228	*22.79 ± 0.46*	*22.35 ± 0.46*	–	–	18.20 ± 0.15

of 6C 1256+36, the flux from which (including associated errors) has been modelled and removed from the *K*-band and F702W data (see Papers I and II of this series, Inskip et al. 2003, 2005). The data for the 6C sources were presented in Paper I (Inskip et al. 2003, which also includes full details of our data reduction methods; the 3CR 4 arcsec diameter aperture magnitudes presented in the current paper were determined using an identical data reduction methodology. With our assumed cosmology, the angular scale at $z \sim 1$ is $\sim$8.6 kpc arcsec^{-1}; this varies by less than $\sim$10 per cent over the redshift range of our data, and we therefore study essentially the same physical aperture size at all redshifts. This 4-arcsec aperture is also large enough that we rarely exclude any emission due to the alignment effect, and that the effects of the seeing remain negligible. The data of Best et al. (1997b) have been supplemented by *H*-band observations of nine 3CR sources, obtained via the UKIRT service observing programme; these data were analysed identically to our other infrared observations, and the resulting 4-arcsec magnitudes are also presented in Table 1.

All 11 6C sources have been observed with one filter of either F702W or F814W. The majority of the $z \sim 1$ 3CR sources studied by Best et al. (1997b) were also observed in one of these two filters. These broad-band filters roughly correspond to ground-based filters in the *UBVRI* system as follows: F814W $\approx I + 0.07(V - I)$, and F702W $\approx R - 0.3(V - R)$. In order to consistently compare the rest-frame UV–optical colours of the host galaxies of 6C and 3CR radio sources at $z \sim 1$, magnitudes through the same filters must be obtained for both full samples. For the galaxies which have not been observed in either the F702W or F814W filters, magnitudes in these filters have been estimated using the observations made in other filters.

For the 14 3CR and eight 6C sources for which high-quality spectra are available (Best et al. 2000a; Inskip et al. 2002b), the following method has been used to determine the F702W and F814W filter magnitudes for cases where no observations in the relevant filter exist. Using the spectroscopic observations, the continuum flux density levels were compared at the mean wavelengths of an observed filter and the filter for which a magnitude was to be determined. By comparing the relative flux levels of the continuum at these wavelengths, and accounting for the different filter widths, the flux in the unobserved filter can be estimated and converted to a magnitude (including the appropriate emission-line contribution for that filter).

This method assumes that the percentage contributions of emission lines, host galaxy and aligned emission does not vary significantly between the region of sky covered by the extracted spectra (a 1.5- to 2.5-arcsec slit aligned along the radio source axis) and the 4-arcsec apertures used for our photometry. The emission-line imaging data obtained by McCarthy et al. (1995), which include a subset of our $z \sim 1$ 3CR sources, support this assumption. For the sources in question, the surface profiles of the line emission and broad-band emission are generally very similar within the aperture size in question. In addition, the bulk of the rest-frame UV excess (both line and continuum emission) lies along the radio source axis and therefore within our spectroscopic slit (see Best et al. 1997b and Inskip et al. 2003 for details); the flux levels in the remainder of our 4 arcsec diameter apertures are generally at a substantially lower level, and any discrepancy will therefore not be a major source of error. We have analysed the spatial variation of the emission-line contribution for two of the 6C sources which displayed particularly extensive emission-line regions (6C 0943+39 and 6C 1129+37; see Inskip et al. 2003, for full details). While the emission-line percentage in the outer regions does vary (e.g. 39.5 per cent of the flux in the outer regions of 6C 0943+39 can be accounted for by line emission, cf. 17.5 per cent line emission in the central 4 arcsec of the spectroscopic data), the overall levels of emission outside the central regions of the slit are much lower. Given the observed distribution of line emission around radio galaxies, we expect that no more than 20 per cent of the total line flux in the 4 arcsec diameter apertures lies outside the regions covered by our long-slit spectroscopy. In order to account for any variations in the percentage contribution of line emission in these regions, we therefore assign an additional 10 per cent error to our calculated emission-line percentages (i.e. allowing for a worst-case scenario error of 50 per cent on the emission-line flux in these regions).

By considering filters as close in wavelength to F702W or F814W as possible, any variation with wavelength in the flux emitted by the aligned structures should be minimized, and will not significantly detract from the accuracy of the estimated magnitudes.

Where sources were observed using more than one *HST*/WFPC2 filter, the flux in the unobserved F702W or F814W filter was estimated using the above method with both of the observed filters, providing these were close in wavelength to the filter in question. The two resulting F702W or F814W magnitudes obtained in this way were very consistent (typically to within 5–10 per cent), and the average value was taken.

In the case of the galaxies for which high signal-to-noise ratio spectra were not available, the relative continuum levels and emission line fluxes of the composite spectra presented in Inskip et al. (2002b) were used instead. Once again, this process was repeated for all the *HST*/WFPC2 filters used in the observations of a given galaxy which were close in wavelength to F702W or F814W. Overall, while the precision of the estimated magnitudes is necessarily lower than that of those which were directly observed, we are confident that this method does produce accurate values.

2.3 Emission-line corrections

We have also endeavoured to determine emission-line percentages in each filter (Table 2). For the eight 6C and 14 3CR sources in our spectroscopic samples, emission-line percentages in the F702W and F814W filters are determined directly from our deep optical spectroscopy (Best et al. 2000a; Inskip et al. 2002c). For other sources, we make use of lower signal-to-noise ratio spectra in the literature (see references in Best et al. 1997; Inskip et al. 2003, for details). Where the spectroscopic data for a given source are of poor quality or do not cover the full wavelength range required (in other words, where we do not have accurate relative fluxes for the full complement of emission lines required), we couple the known line strengths of major emission lines such as [O II] 3727 Å with the composite emission-line ratios of Inskip et al. (2002b), which were determined based on the spectra of 14 3CR and eight 6C sources at $z \sim 1$. These composite spectra provide typical emission-line ratios (including errors) for both large and small radio sources in each sample; by using the most appropriate line ratios for a given source we can therefore account for the expected variations in the ionization state of the emission-line gas due to differences in radio source properties (power and size) within the samples. This method of correcting the galaxy colours for emission-line contamination does however assume that the distribution of line and continuum emission within the apertures is similar (as noted in the preceding section); any errors introduced by such a discrepancy are likely to be small ($\sim$10 per cent) and are included in the uncertainties on each value. This uncertainty is combined with the inherent errors in flux calibration for the spectra, the uncertainties in the continuum level for the filter, plus the errors associated with any line ratios derived from

Table 2. The emission line and unresolved point source percentages for each filter (where known). The emission-line data were previously presented for these sources in Inskip et al. (2002b), and Best et al. (2000a); analysis of the emission-line contributions in the directly observed filters can be found in Inskip et al. (2003) and Best et al. (1997) (see text for details of the emission-line corrections for the remaining data). Our analysis of the nuclear point source contributions is presented in Inskip et al. (2005) and Best et al. (1998). Also listed are the emission-line-corrected (i.e. continuum) galaxy colours, and their associated errors, derived from the magnitudes in Table 1 and the emission-line contributions listed below. The *HST*/WFPC2 filter colours can be approximated to ground-based UBVRI colours as F702W-K $\approx (R-K) - 0.15$ and F814W-K $\approx (I-K) + 0.05$.

Source	Emission-line percentages[a]					Nuclear point source percentages			Emission-line-corrected (i.e. continuum) colours			
	F702W	F814W	J^a	H^a	K^a	F702W	F814W	K	F702W$-K$	F814W$-K$	$J-K$	$H-K$
6C 0825+34	3 ± 1	3 ± 2	25	28	5	–	–	–	3.44 ± 0.36	2.95 ± 0.25	0.93 ± 0.32	0.78 ± 0.42
6C 0943+39	18 ± 5	21 ± 4	1	0	0	36 ± 4	–	41.5 ± 3.5	4.21 ± 0.17	3.72 ± 0.21	1.62 ± 0.14	1.18 ± 0.16
6C 1011+36	8 ± 4	9 ± 1	3	0	0	25 ± 2	–	28.8 ± 1	3.99 ± 0.10	3.50 ± 0.16	1.88 ± 0.21	0.80 ± 0.12
6C 1017+37	17 ± 4	22 ± 3	14	1	0	12 ± 3	–	4^{+18}_{-4}	3.40 ± 0.11	2.80 ± 0.17	1.46 ± 0.23	0.98 ± 0.18
6C 1019+39	5 ± 1	5 ± 1	2	0	0	–	0 ± 1	0 ± 1	4.30 ± 0.29	3.33 ± 0.06	1.69 ± 0.08	0.91 ± 0.07
6C 1100+35	5 ± 1	7 ± 4	35	28	3	–	$41^{+11}_{-1} \pm 2$	15 ± 14	4.35 ± 0.27	3.86 ± 0.10	1.89 ± 0.36	1.27 ± 0.30
6C 1129+37	15 ± 5	25 ± 4	1	0	0	–	–	18 ± 1	4.39 ± 0.11	4.14 ± 0.17	1.55 ± 0.13	0.50 ± 0.11
6C 1204+35	7 ± 2	11 ± 7	56	50	8	–	–	13 ± 1	3.82 ± 0.30	3.33 ± 0.17	1.70 ± 0.51	1.11 ± 0.47
6C 1217+36	2 ± 1	3 ± 1	0	0	0	–	23 ± 5	25 ± 0.5	4.38 ± 0.26	3.37 ± 0.08	1.95 ± 0.13	0.96 ± 0.09
6C 1256+36	9 ± 4	15 ± 3	0	0	0	0	–	0 ± 3	5.02 ± 0.12	4.64 ± 0.17	1.60 ± 0.21	0.44 ± 0.21
6C 1257+36	9 ± 1	10 ± 2	28	0	0	–	$3.5^{+1}_{-3.5} \pm 2$	16 ± 0.5	4.15 ± 0.30	3.59 ± 0.07	2.16 ± 0.29	0.77 ± 0.09
3C 13	8 ± 2	19 ± 4	95	–	17	–	–	0^{+7}_{-0}	3.65 ± 0.32	3.16 ± 0.21	1.82 ± 0.76	–
3C 22	10 ± 1	19 ± 1	45	2	0	–	–	50^{+20}_{-10}	4.44 ± 0.16	3.86 ± 0.05	2.27 ± 0.41	1.31 ± 0.11
3C 34	1 ± 1	1 ± 1	0	–	0	–	–	5^{+6}_{-0}	4.25 ± 0.26	3.58 ± 0.26	1.84 ± 0.13	–
3C 41	15 ± 2	11 ± 2	38	–	0	–	–	31^{+10}_{-8}	4.68 ± 0.21	4.01 ± 0.21	3.24 ± 0.38	–
3C 49	17 ± 3	8 ± 2	–	–	0	–	–	0^{+2}_{-0}	3.90 ± 0.16	3.17 ± 0.08	–	–
3C 65	8 ± 2	5 ± 1	0	–	0	–	–	0^{+8}_{-0}	4.96 ± 0.19	3.92 ± 0.11	1.73 ± 0.17	–
3C 68.2	4 ± 1	4 ± 1	38	–	0	–	–	–	4.21 ± 0.34	3.71 ± 0.34	1.94 ± 0.45	–
3C 217	31 ± 3	20 ± 1	84	9	0	–	–	0^{+6}_{-0}	3.22 ± 0.21	2.63 ± 0.13	1.59 ± 0.69	1.20 ± 0.28
3C 226	14 ± 2	10 ± 1	29	3	0	–	–	13^{+8}_{-13}	3.77 ± 0.20	2.91 ± 0.18	1.91 ± 0.31	1.02 ± 0.16
3C 239	11 ± 3	6 ± 1	3	–	1	–	–	–	3.81 ± 0.24	3.32 ± 0.13	1.13 ± 0.19	–
3C 241	1 ± 1	8 ± 2	3	–	0	–	–	–	4.38 ± 0.24	3.89 ± 0.14	1.40 ± 0.21	–
3C 247	11 ± 1	15 ± 1	–	–	0	–	–	–	4.42 ± 0.25	3.60 ± 0.06	–	–
3C 252	7 ± 1	11 ± 1	–	–	0	–	–	17^{+7}_{-17}	3.63 ± 0.17	3.17 ± 0.11	–	–
3C 265	22 ± 2	18 ± 2	56	8	0	–	–	8^{+4}_{-8}	3.34 ± 0.25	2.85 ± 0.31	1.90 ± 0.49	1.21 ± 0.15
3C 266	10 ± 1	16 ± 1	–	–	9	–	–	4^{+9}_{-4}	3.25 ± 0.17	2.66 ± 0.17	–	–
3C 267	8 ± 2	12 ± 2	1	–	1	–	–	0^{+5}_{-0}	4.12 ± 0.12	3.60 ± 0.15	1.74 ± 0.19	–
3C 277.2	23 ± 3	9 ± 2	20	–	0	–	–	15^{+6}_{-15}	3.08 ± 0.22	2.60 ± 0.10	1.47 ± 0.25	–
3C 280	15 ± 2	20 ± 1	51	0	0	–	–	0^{+8}_{-0}	4.02 ± 0.11	3.48 ± 0.09	1.88 ± 0.47	1.05 ± 0.17
3C 289	8 ± 1	10 ± 1	28	0	0	–	–	1^{+6}_{-1}	4.51 ± 0.11	3.55 ± 0.10	1.87 ± 0.31	0.91 ± 0.17
3C 324	7 ± 1	14 ± 2	4	17	9	–	–	0^{+4}_{-0}	4.15 ± 0.14	3.56 ± 0.24	1.80 ± 0.22	1.05 ± 0.27
3C 337	7 ± 1	5 ± 1	0	–	0	–	–	2^{+7}_{-2}	4.02 ± 0.26	3.16 ± 0.08	1.61 ± 0.14	–
3C 340	12 ± 1	18 ± 2	19	3	0	–	–	0^{+4}_{-0}	3.92 ± 0.20	2.81 ± 0.23	1.63 ± 0.24	0.84 ± 0.15
3C 352	22 ± 2	13 ± 1	–	–	0	–	–	7^{+6}_{-7}	3.76 ± 0.12	3.20 ± 0.09	–	–
3C 356	10 ± 1	13 ± 1	–	–	0	–	–	0^{+14}_{-0}	3.78 ± 0.14	3.21 ± 0.11	–	–
3C 368	10 ± 1	12 ± 1	3	2	4	–	–	–	3.37 ± 0.11	2.46 ± 0.13	1.83 ± 0.16	0.64 ± 0.17
3C 437	3 ± 1	5 ± 1	–	–	3	–	–	–	4.15 ± 0.34	3.65 ± 0.34	–	–
3C 441	6 ± 1	10 ± 1	0	–	0	–	–	0^{+5}_{-0}	3.64 ± 0.17	2.89 ± 0.17	1.66 ± 0.12	–
3C 470	14 ± 2	8 ± 2	–	–	0	–	–	–	4.73 ± 0.48	4.23 ± 0.48	–	–

[a]The infrared emission-line contributions are derived from appropriate emission-line ratios and the observed fluxes of [OII] 3727 Å and Hβ, and are given as a rough estimate only, as they are only believed to be accurate to about a factor of 2 (see text for details). An error of 50 per cent on the calculated emission-line contribution to the *JHK* magnitudes has been included in our calculation of the error on the emission-line-corrected galaxy colours.

composite spectra where applicable (see Best et al. 2000a and Inskip et al. 2002b for further details of the errors involved).

Given the evidence that emission-line flux scales with radio power (e.g. Rawlings & Saunders 1991; Willott et al. 1999; Jarvis et al. 2001; Inskip et al. 2002c), one might expect the line emission from the 6C sources to be lower by a factor of $\sim$6 than that of the 3CR sources at the same redshift, and therefore to account for a lower fraction of the total UV excess observed. However, the choice of broad-band *HST* filters for these observations was such that the wavelength of the dominant [O II] emission line is at a higher filter throughput for the 6C observations than the 3CR observations. As this is the most prominent emission line in the rest-frame UV spectra of these galaxies, the emission-line contribution to the *HST* magnitudes for the 6C sources, although still less on average than

the 3CR emission-line contribution, is higher than might otherwise be expected (Inskip et al. 2003).

As we do not have high-quality spectra at longer wavelengths for the galaxies in our $z \sim 1$ samples, J, H, K emission-line percentages have been estimated using standard optical emission-line ratios (Osterbrock 1989; McCarthy 1993), determined relative to measured fluxes for Hβ and/or [O II]. While our spectroscopic data are certainly subject to slit losses, we simultaneously consider the total flux within the J, H, K and F702W/F814W filters. This allows us to correctly balance the relative contributions of line and continuum emission in different wavelength ranges, in accord with our the observations, thus avoiding any potential systematic errors due to a mismatch between line and continuum flux in different filters. Unfortunately, whilst being free of most sources of systematic error, one problem remains, and our estimation of the emission-line fluxes in the observed-frame infrared based on existing optical spectra is not likely to be particularly accurate compared to that for the emission lines lying at shorter wavelengths. This is due to the fact that there is considerable variation in emission-line ratios with radio source size and power (e.g. Inskip et al. 2002b), which cannot be adequately accounted for using a single set of line ratios for the full sample. Therefore, based on the known variations in these line ratios at shorter wavelengths, the uncertainties in these values are easily of the order of a factor of 2. Whilst this may seem to be a significant factor, the overall emission-line corrections in the observed J, H, K wavebands are typically small, and therefore the errors on the observed magnitudes will not be greatly degraded in most cases. Nonetheless, in point of this fact, throughout this paper we display the resulting galaxy colours both with and without emission-line correction. The resulting emission-line percentages are presented in Table 2, together with the nuclear point source percentages determined in Inskip et al. 2005 (Paper II, this series) and Best et al. (1998). The emission-line-corrected galaxy colours and their associated errors (calculated from the errors on the 4-arcsec aperture magnitudes and the errors on the emission-line contribution in each filter) are also presented in Table 2.

3 RESULTS

3.1 Observed F702W-K and F814W-K galaxy colours

Fig. 1 displays the uncorrected F814W-K and F702W-K colours (derived directly from the data in Table 1) for the 6C and 3CR sources as a function of redshift, the galaxy colours after removal of the emission-line contributions in each filter (see Table 2), and the corrected data binned in equal redshift intervals. The model tracks were created using the spectral synthesis models of Bruzual & Charlot (2003), and represent passively evolving old stellar populations which were formed in an instantaneous burst at redshifts ranging from $z = 3$ to 20. Correcting for line emission does not greatly alter the overall picture. The colours of the 6C sources with the weakest alignment effect (e.g. 6C 1019+39 at $z = 0.922$ and 6C 1256+36 at $z = 1.128$) display corrected colours consistent with passively evolving old stellar populations (i.e. the tracks plotted in Fig. 1); similar results are observed for the 3C sources with a weak alignment effect. In all other cases, the remaining sources retain their blue colours after emission-line correction, suggesting that line emission does not dominate the alignment effect. The blue colour of 6C 1217+36 ($z = 1.088$), which has also has no obvious alignment effect, can be attributed to a clear UV excess lying within the bounds of the host galaxy (Inskip et al. 2005).

A further complicating factor is the fact that several sources are known to have a fairly strong contribution to the flux in one or more filters from an unresolved nuclear point source. Corrections for any nuclear point source contribution have not been made, as the data are not sufficiently deep in all filters for accurate corrections for nuclear point source emission to be carried out for all sources in all filters. For the sources with a measured point source contribution in more than one filter, it is possible that a power-law model could be applied in order to derive the point source contribution in other filters. However, such an approach would be fraught with error for the sources with large errors on their point source contributions, or a measured point source in only one filter, and would not be possible at all for the many sources for which such measurements have not been possible. Additionally, it is quite plausible that any unresolved nuclear point source may be due in part to recent star formation in the central regions of the host galaxy (cf. the 4 kpc diameter ring of young stars observed in Cygnus A: Fosbury et al. 1999), thus rendering any attempt at such modelling useless at this stage. Whilst we cannot fully correct for any point source contribution, it is of importance to hold such effects in consideration throughout the analysis of these data. For the majority of sources, the point source contributions are either relatively weak, and/or comparable in all filters in which they were measurable. However, stronger nuclear emission (>30 per cent in one or more filters) is observed for several sources (6C 0943+39, 6C 1100+35, 3C22, 3C41). For these sources, we cannot accurately gauge the influence of nuclear point source emission on the resulting galaxy colours. In order not to bias our results, these four sources are excluded from any statistical analysis, as well as the histogram plots of the galaxy colours (Figs 2 and 4).

The data for both colours vary similarly with redshift. At the lowest redshifts (where the alignment effect is generally weaker), the galaxy colours are consistent with the predictions for passively evolving galaxies. Out to $z \sim 1.1$–1.3, the passive evolution tracks become redder whilst the observed galaxy colours remain roughly constant (as can be seen from the binned data plotted in the bottom panels of Fig. 1). This reflects the increasing importance of the excess UV emission associated with the alignment effect at these redshifts, and indicates a clear evolution of the galaxy properties over these redshifts. At higher redshifts, the average colours then increase, and the galaxies become redder. In order to explain the variation of these colours at high redshifts, it is useful to consider the changing rest-frame wavelengths sampled by the *HST*/WFPC2 filters. At $z \sim 1$, the rest-frame wavelengths for the F702W and F814W filters are ∼3500 and ∼4000 Å, respectively; at $z \sim 1.5$ these become ∼2800 Å for F702W and ∼3200 Å for F814W. Although the old stellar population of a galaxy will be younger at $z \sim 1.5$ than at $z \sim 1$ (and therefore bluer in colour), a galaxy at $z \sim 1.5$ is far less luminous at the rest-frame wavelength of the observations than a galaxy at $z \sim 1$: emission longwards of the 4000-Å break passes beyond the F702W filter at $z \sim 1$, and the F814W filter at $z \sim 1.3$. Given that the relative change in K-band flux is much less, this explains the observed increase in the F814W-K and F702W-K colours at $z \gtrsim 1.1$–1.3.

Unlike the 3CR sources, the 6C galaxies are restricted to a narrower redshift range closer to $z = 1$. With the observed variation in galaxy colours with redshift, any comparison between both full samples would automatically lead to bluer colours on average for the 6C sources. To avoid any confusion, further analysis of the 3CR sources is restricted to in the redshift range overlapping with the 6C subsample, $0.85 < z < 1.5$. Fig. 2 displays the distribution of the corrected F814W-K and F702W-K colours for the galaxies in both samples in this redshift range as two histograms.

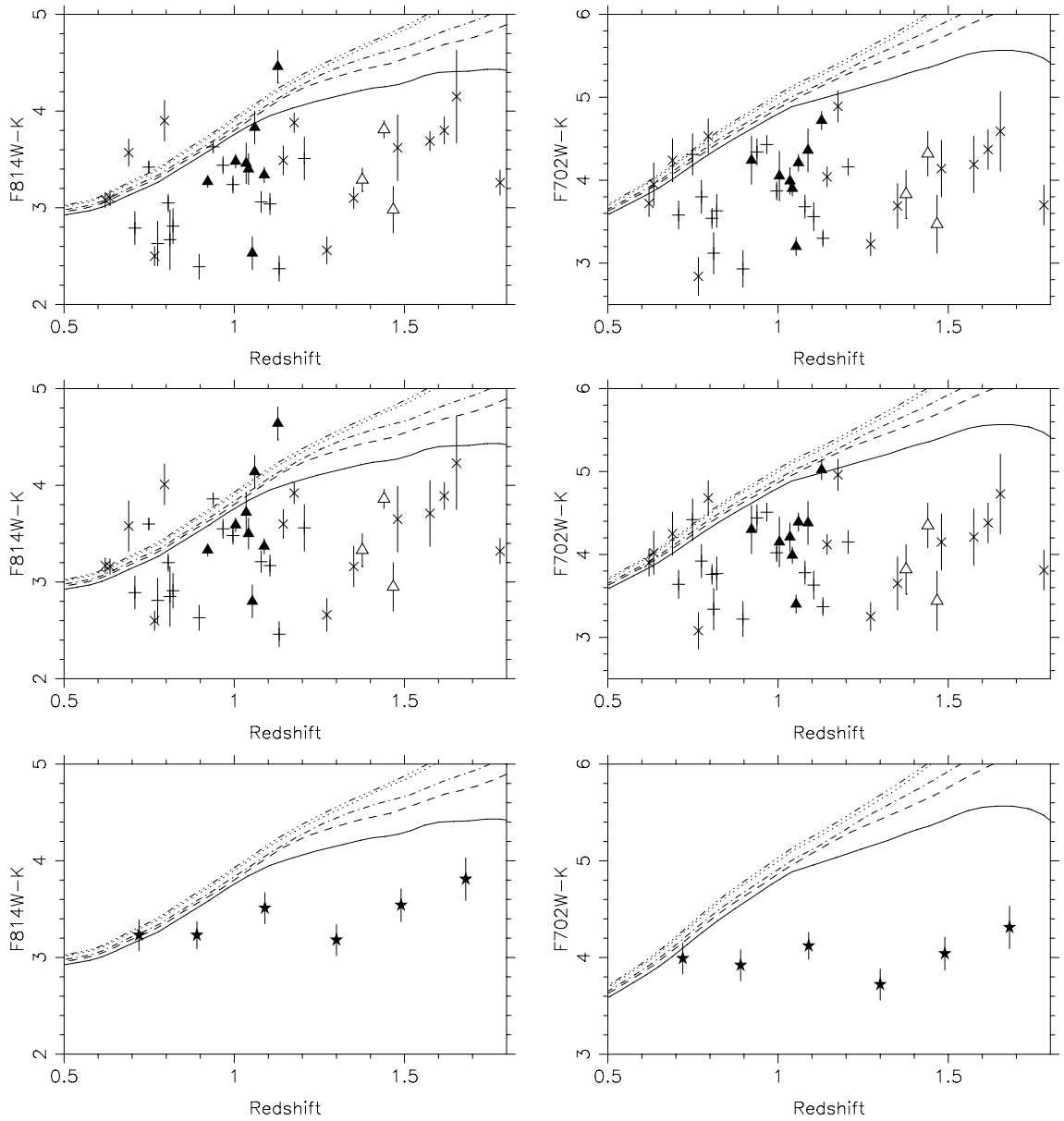

Figure 1. Top row: observed 4-arcsec F814W-K (left-hand panel) and F702W-K (right-hand panel) colours versus redshift for 6C and 3CR radio galaxies. Middle row: 4-arcsec F814W-K and F702W-K colours after correcting for both *K*-band point source contributions and also emission-line contamination. Bottom row: the same (corrected) data binned in equal redshift intervals. 6C sources are represented by the triangles: filled triangles represent the eight sources in the $z \sim 1$ spectroscopic sample. 3CR sources are represented by crosses: the sources in the 3CR $z \sim 1$ spectroscopic sample are marked by '+', with the remaining galaxies marked by '×'. Error bars represent the standard error on the mean value. The tracks represent the F814W-K and F702W-K colours for passively evolving elliptical galaxies formed at redshifts of 3 (solid line), 4 (dashed line), 5 (dot–dashed line), 10 (dotted line) and 20 (dot–dot–dot–dashed line).

The distribution of the F814W-K colours appears to be similar for the galaxies in both subsamples. The mean value of F814W-K is slightly redder for the 6C sample by ∼0.25 mag. The F702W-K colours are almost identical for both samples, with the mean 6C colour being ∼0.2 mag redder than that for the 3CR sources. Kolmogorov–Smirnov tests show that the typical galaxy colours of the two samples are not significantly different. The fact that the two samples display such similar colours is particularly surprising. With so many alignment effect mechanisms closely linked to the properties of the radio source, the luminosity of the extended structures at the wavelengths of the *HST* observations might be expected to be greater relative to the host galaxy emission observed in the *K* band for the more powerful 3CR radio sources, leading to bluer F702W-K and F814W-K colours. The similarity in colours between the two samples suggests that this is not the case, and that a more detailed consideration of the effects of the radio source properties on the different types of aligned emission features is required.

3.2 Galaxy colours in the infrared

In addition to our 6C data, *J*-band magnitudes are available for 20 of the 28 3CR galaxies in the $z \sim 1$ subsample, and *H*-band data are also available for nine of these sources. Fig. 3 displays the observed $J - K, H - K$ and $J - H$ colours for the 6C and 3CR galaxies as a

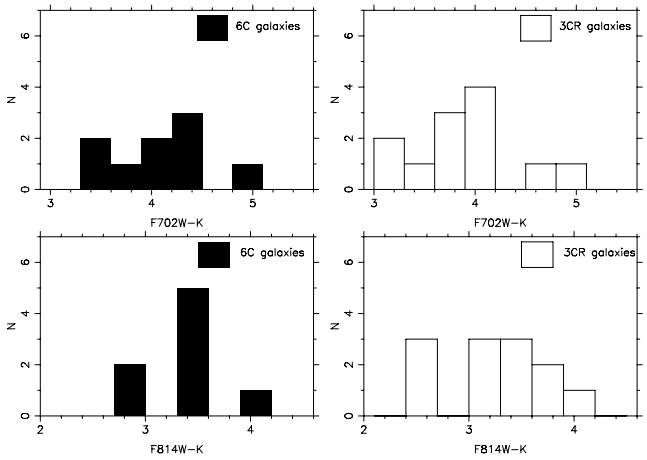

Figure 2. Histogram of observed 4-arcsec F702W-K (top) and F814W-K (bottom) colours for the 6C (left-hand panels) and 3CR (right-hand panels) galaxies in the redshift range $0.85 < z < 1.5$. The 6C sources are represented by the black boxes, and the 3CR sources by the white boxes.

function of redshift together with the tracks for passively evolving elliptical galaxies. We also display the same data after correcting for the (estimated) emission-line contribution. Histograms displaying the variation in colour for each sample over the redshift range of the 6C data ($0.85 < z < 1.5$) are displayed in Fig. 4. The data for both the 6C and 3CR subsamples are clearly seen to span the same range of colours.

The majority of infrared emission for galaxies at these redshifts (excluding line emission) is believed to be due to the old stellar populations of the host galaxies, and most sources do indeed lie on or close to the tracks for passively evolving old stellar populations, as would be expected. There is no clear difference between the 6C and 3CR colours, either before or after emission-line correction. However, emission-line correction does move the sources with the bluest observed colours back towards the predictions of passive evolution models. Assuming that the stellar populations of the radio source host galaxies all formed at approximately the same cosmic epoch, there is little difference in the expected spectral energy distribution (SED) between galaxies at $z \sim 1$ and those at $z \sim 1.5$ except that due to their younger age, the more distant sources are expected to be intrinsically slightly brighter. However, the change in rest-frame wavelength for galaxies observed at these epochs is such that the more distant sources will be observed to have a bluer $J - K$ colour, due to an additional small contribution of aligned emission to the J-band magnitudes of the higher-redshift sources. This is indeed the case for our $J - K$ and $J - H$ colours at $z > 1.2$. The long-wavelength tail of the alignment effect will not contribute so strongly (if at all) for emission observed in the longer-wavelength H and K filters.

4 INTERPRETING THE GALAXY COLOURS

Although the colours of the galaxies in the 6C and 3CR $z \sim 1$ samples are very similar, this certainly does not imply that they are similarly luminous in any given waveband. Indeed, it is clear that this is not the case. In the K band (which at $z \sim 1$ is dominated by emission from the old stellar populations of the host galaxies), the 6C sources are $\sim$0.6 mag fainter than the 3CR sources at the same redshift (Inskip et al. 2002a). Similar trends are apparent from our shorter wavelength *HST* observations (Inskip et al. 2003). The similarity in observed infrared colours, regardless of luminosity, is to be expected: at these wavelengths, the emission from the galaxies in both samples is dominated by their passively evolving old stellar populations. However, their observed optical colours are also statistically identical. This result is more surprising, as the more powerful 3CR sources might be expected to display a stronger alignment effect (and therefore bluer colours). There are two possible explanations: either the alignment effect is not radio power dependent, or some additional process is working to counterbalance the expected bluer colours of the 3CR sources. In this section, we will investigate the likely causes of this result.

When considering the differences between different galaxy populations, it is of essential importance that all possible sources of bias are considered. This is particularly true for radio galaxies, where the properties of the radio source are often closely tied to those of its host galaxy. Environmental effects may be an important factor in determining the overall size and luminosity of a radio source of a given power. Observational evidence suggests that the very largest (>1-Mpc) radio sources are expanding more rapidly than average into a below-average density intergalactic medium (IGM, e.g. Cotter 1998; Mack et al. 1998), and may be of similar age to more typical sources of several hundred kpc in extent. Evidence for intermittency in the radio source activity for these largest radio sources (which, given their age, may be most likely to display it) is rare (e.g. Lara et al. 2004). For radio sizes typical of those in our $z \sim 1$ subsamples, spectral and dynamical ages are in good agreement up to ages of the order of 10^7 yr (e.g. Blundell & Rawlings 2000), but the argument that a larger source size corresponds to a greater age, while not a 1:1 correspondence, at least holds true as a solid first approximation for sources over the full range of sizes. At the smallest end of the scale, whilst not all compact radio sources (i.e. compact steep spectrum/gigahertz peaked spectrum, hereafter CSS/GPS, sources) will necessarily evolve into larger FR II radio sources, it is most likely that these are genuinely young objects (e.g. Fanti et al. 2000; Tzioumis et al. 2002; Ojha et al. 2004) rather than older sources 'frustrated' by a dense interstellar medium (O'Dea 1998, and references therein).

Within a single flux-limited sample, the higher redshift sources are not only more powerful (due to Malmquist bias), but also have a smaller average size (and therefore younger average age). This is due to the fact that radio luminosity decreases with source size; sources which meet the selection criteria for the sample when small will not necessarily do so at larger radio sizes (Neeser et al. 1995; Kaiser, Dennett-Thorpe & Alexander 1997; Blundell, Rawlings & Willot 1999.) As a consequence of this, the largest radio sources in any given redshift range will host (on average) intrinsically more powerful AGN than their smaller counterparts. We bear these issues in mind as we consider the variations in galaxy colours as a function of radio source size and power.

4.1 The importance of radio source size

A possible explanation for the unexpectedly blue F702W-K and F814W-K colours displayed by the 6C sources is that the average projected radio size of the sources in the 6C sample ($\sim$150 kpc) is less than that for the 3CR sources in the same redshift range ($\sim$ 230 kpc). Given the observed trend for smaller radio sources to display a more extreme alignment effect (e.g. Best et al. 1996; Inskip, Best & Longair 2004), any correlation between radio size and galaxy colour could then lead to a bluer average colour for the 6C sources than would be expected if both samples had the same mean radio size. The variation in these colours with radio source size is an essential consideration; plots of the corrected colours versus

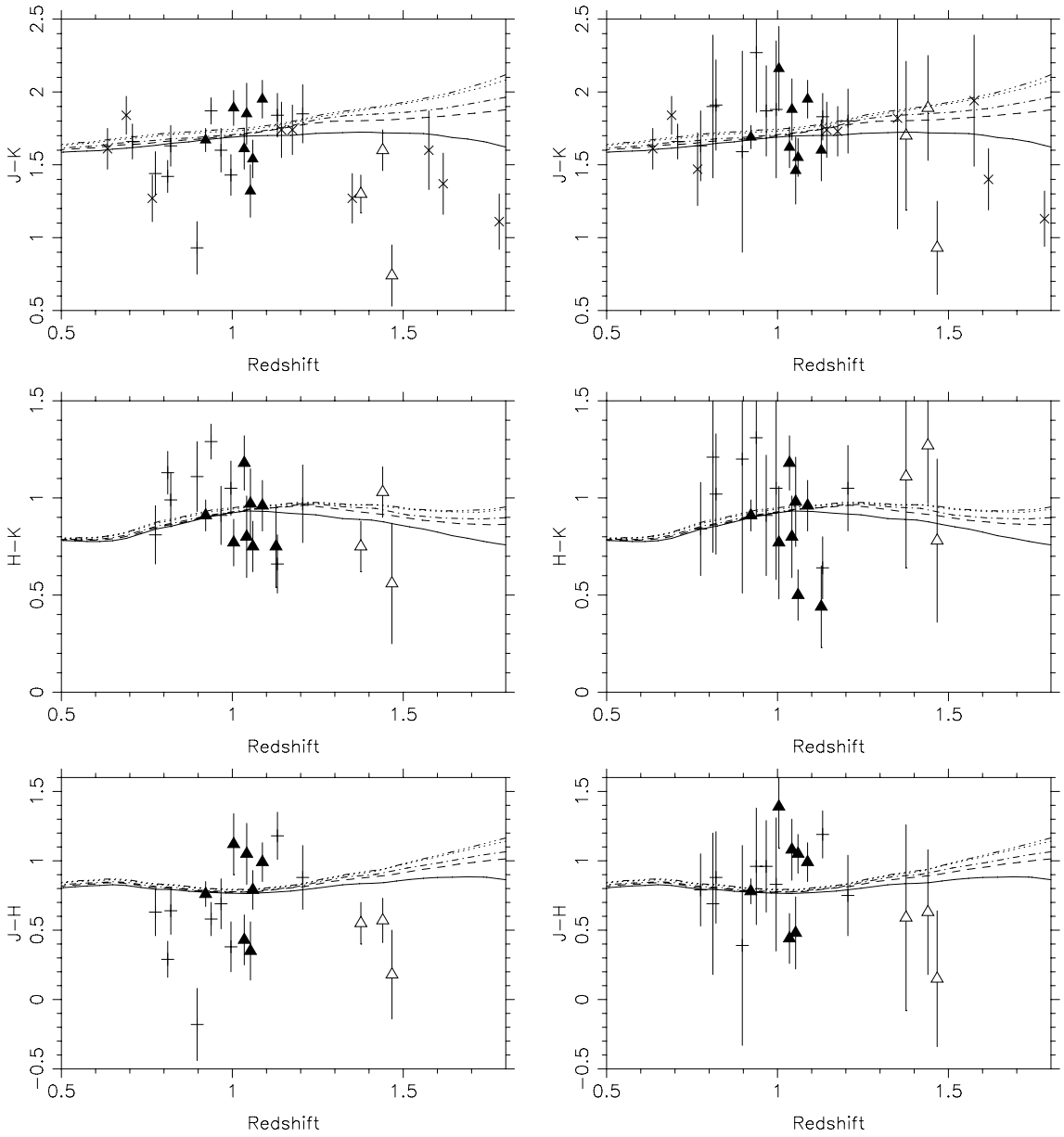

Figure 3. Observed (left-hand panels) and corrected (right-hand panels) 4 arcsec $J - K$ (top), $H - K$ (centre) and $J - H$ (bottom) colours versus redshift for the 6C and 3CR galaxies at $z \sim 1$. The tracks represent the $J - K$ colours for passively evolving elliptical galaxies, formed at redshifts of 3 (solid line), 4 (dashed line), 5 (dot–dashed line), 10 (dotted line) and 20 (triple-dot–dashed line). Symbols are as in Fig. 1. 3C41, which is thought to have a point source quasar contribution to its K-band emission (Best et al. 1997b), has an extremely red $J - K$ colour of 2.89 and lies off the plot.

radio size are displayed in Fig. 5. Also displayed in Fig. 5 is the distribution of $J - K$colours with radio size for the two samples. These data do not show any signifcant correlation with radio size; neither do our data in the other infrared (IR) colours. In general this is as expected, as radio size should not have any influence on the properties of the old stellar population.

As already noted, the distribution of radio sizes within the two $z \sim 1$ samples is quite different. Therefore, for a fair comparison between the sources in the 6C and 3CR samples in this redshift range, it is justified to first consider only the smaller radio galaxies, i.e. those with a radio size $<$200 kpc, for which the two samples display a similar distribution of projected sizes. There is no difference between the mean F702W-K and F814W-K colours in each sample over this range of radio sizes. In this size range, excluding the sources with large point source contributions, the data sets for both colours (corrected for emission-line contamination) are correlated with radio source size at significance levels of $\sim$97.5 and $\sim$95 per cent in a Spearman Rank correlation test for the F814W-K and F702W-K colours, respectively. The strong correlation between galaxy colour and projected radio source size for these data is matched by the behaviour of many other properties of these systems, which display the greatest variety over this range of radio sizes (Inskip et al. 2002b, 2004).

However, a visual inspection of the plots suggests that this trend does not hold true out to the largest radio sizes within our sample, and has certainly broken down for sources larger than $\sim$400 kpc. Considering sources up to 400 kpc in size, the corrected F814W-K colours are found to be correlated with radio size at a reduced

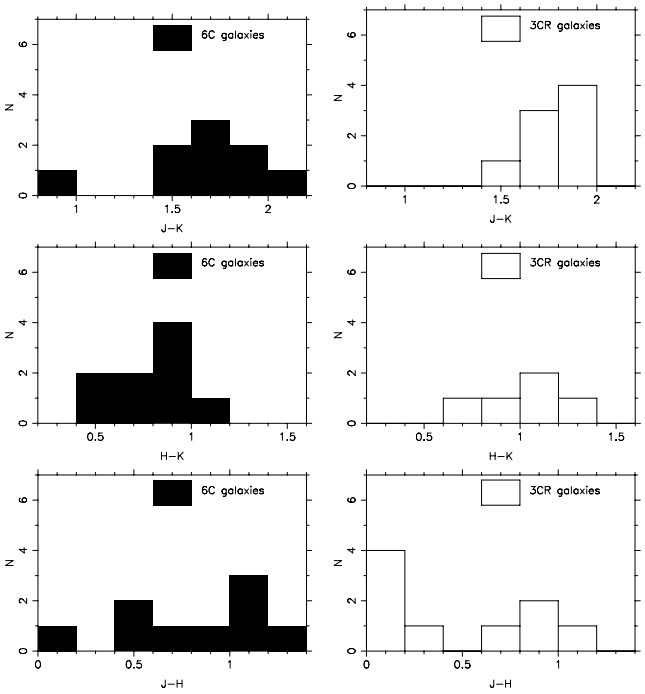

Figure 4. Histogram of observed 4 arcsec $J-K$ (top) and $H-K$ (bottom) colours for the 6C (left-hand panels) and 3CR (right-hand panels) galaxies in the redshift range $0.85 < z < 1.5$. The 6C sources are represented by the black boxes, and the 3CR sources by the white boxes. Both subsamples display a similar range of colours.

significance level of >97.5 per cent, and no statistically significant correlation is observed for F702W-K. For the full sample, the correlation for the corrected F814W-K colours is further weakened (with a significance level of ∼95 per cent). It is also worth noting that the radio size correlations have an increased significance prior to emission-line correction; this is due to the known strong correlation between emission-line flux and radio source size in these sources (Inskip et al. 2002c).

These results are generally exactly as expected; smaller radio sources typically display brighter, more extensive aligned emission (Best et al. 2000b; Inskip et al. 2003). As illustrated by the case of 6C 1257+36 (Inskip et al. 2003; Paper I), at the wavelengths of the *HST* observations the aligned emission for sources of all radio source sizes is generally bluer than the host galaxy itself.

There are no obvious reasons why the very largest sources ($D_{\rm rad} > 400$ kpc) in both $z \sim 1$ samples should have colours as blue as those observed, which goes against the strong trend with radio size observed for the smaller sources. One possible explanation is that these largest sources may exist in a very much less dense IGM, and may have ages (and therefore colours) more comparable to the smallest sources in our sample. However, two of these three sources (6C 1011+36 and 3C 356) appear to have one or more nearby companions (Best 1996; Inskip et al. 2003), as do several other smaller radio sources which also display a more pronounced alignment effect (e.g. 6C 1129+37). These factors could potentially lead to an increase in the interactions between the radio source and the surrounding IGM, above the level expected for the other large sources ($D_{\rm rad} > 120$ kpc) in the sample. Indeed, it has been suggested (Simpson & Rawlings 2002) that the triggering of 3C 356 may have been caused by a violent interaction with a nearby object. It can also be argued that in order for a radio source to survive at high

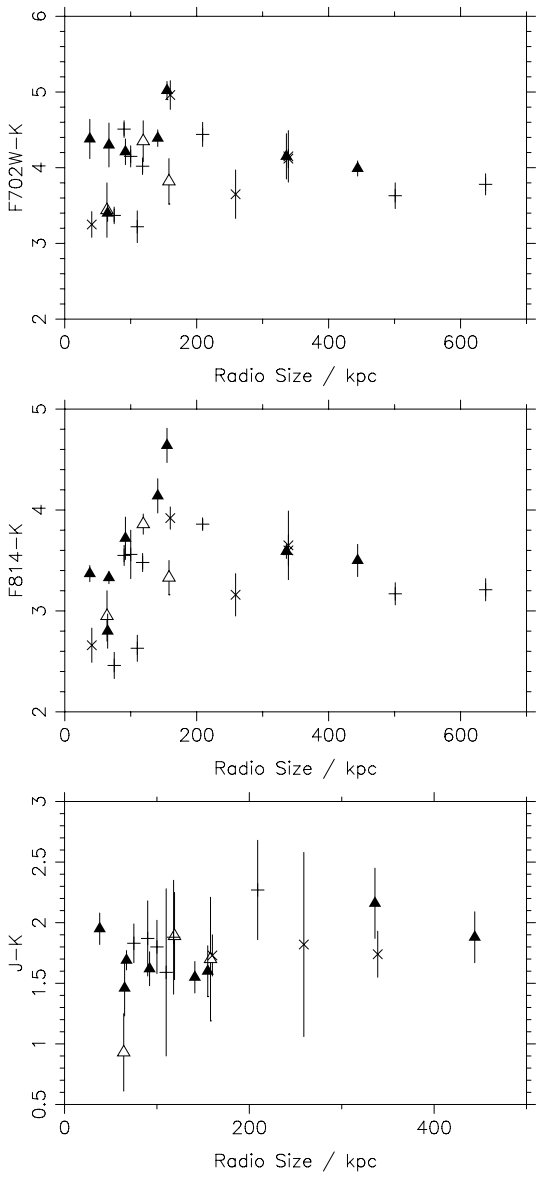

Figure 5. 4-arcsec F702W-K (top), F814W-K (centre) and $J-K$ (bottom) colours (corrected for line emission) versus radio size for 6C and 3CR radio galaxies in the redshift range $0.85 < z < 1.5$. Symbols are as in Fig. 1.

luminosity to such large sizes, it may require a slightly denser IGM (e.g. Kaiser & Alexander 1999) and therefore may be more likely to reside in a richer cluster environment, where interactions are more frequent. Whilst not the norm, interactions are seen in many different sources, over a wide range of redshifts and radio powers (e.g. Smith & Heckman 1989; Lacy et al. 1999; Roche & Eales 2000), often resulting in bluer colours for the host galaxy than would be expected given the predictions of passive evolution models. The faint companion objects nearby many of these blue/interacting systems often seem to display a preference for lying close to the radio source axis (e.g. van Breugel et al. 1998; Roche & Eales 2000; Pentericci et al. 2001). Rigler et al. (1992) also find that small red companion objects are often observed nearby powerful radio sources; although they find no preferential location for these objects, they are generally associated with the radio sources which display the bluest colours and the most extreme alignment effects. Although the most extreme star forming features are only frequently observed at the highest

redshifts, it is certainly plausible that any merger related activity at lower redshifts could easily boost any observed alignment effect above the norm for the cosmic epoch of the source in question. It does seem likely that the anomalous sources within our own two samples also fit this pattern, and suggest that environmental factors are of importance.

4.2 Variations with radio source power

By comparing galaxies of a similar radio size within a fixed redshift range, it should be possible to clearly deduce the influence of radio source/AGN power on the observed properties of these complex systems. The most plausible option for explaining the greater luminosity of the more powerful 3CR sources is a greater mass for their host galaxies. Given the known correlation between black hole mass and galaxy bulge mass (Kormendy & Richstone 1995), a further correlation between galaxy mass and radio source power might be expected, if the black holes were being fuelled at the Eddington limit. However, whilst variations in mass may account for much of the scatter within the two samples, analysis of the galaxy morphologies suggests that radio galaxies are hosted by similar sized galaxies over a wide range of redshifts and radio powers (Inskip et al. 2005, and references therein).

There are several other options by which this luminosity difference between the samples may be explained. First, the more powerful 3CR sources might be expected to display greater AGN contamination in their broad-band fluxes. However, the average unresolved point source contributions for the $z \sim 1$ 6C and 3CR samples are statistically indistinguishable (Inskip et al. 2005, Paper II). Although this result is somewhat surprising, the radio core flux fraction of the 6C data is higher on average than for the 3CR sources at the same redshift (Best et al. 1997b, 1999), suggesting that the sources in our 6C subsample are typically observed at an angle closer to the line of sight than the 3CR sources. This would imply less obscuration of the 6C AGN, and therefore bluer colours/brighter emission than might otherwise be expected. Overall however, AGN contamination cannot account for the luminosity difference between the two samples, nor is it sufficient to explain the similarity in colours between the 6C and 3CR $z \sim 1$ sources.

A second factor is the alignment effect itself, which is particularly luminous in the case of the $z \sim 1$ 3CR sources. The long wavelength tail of the alignment effect is clearly visible in the *J*-band imaging observations of the 3CR data, which reveal a definite contribution of emission from the extended aligned features. At a much lower level, the *K*-band emission of the 3CR sources also displays some extension along the radio source axis. Such features are not observed in our images of the 6C sources, although this could be due to the lower signal-to-noise ratio levels of these observations (Best et al. 1996, 1997b; Inskip et al. 2004). Whilst an alignment effect is only observed in the IR for the more powerful 3CR $z \sim 1$ sources, it is not likely to contribute more than $\sim$10 per cent of the total *K*-band flux for these sources (Rigler et al. 1992; Best et al. 1998; Zirm, Dickinson & Dey 2003). Therefore, excess emission from the long-wavelength alignment effect cannot reconcile the differences in *K*-band emission for the two samples, nor can it account for the fact that high redshift radio galaxies are on average more luminous ($\sim$0.5 mag at $z \sim 1$) than expected based on the predictions of passive evolution models (Inskip et al. 2002a). The only plausible options remaining are to also consider the effects of variations in the radio source environment, and the host galaxy stellar populations. We will now discuss the effects of each of these in turn.

4.2.1 Host galaxy environment

The environments of radio sources vary quite markedly with redshift. Low-redshift radio galaxies are predominantly found in small groups and avoid richer cluster environments, whilst at higher redshifts, a wider range of environments is observed, including richer groups and clusters (e.g. Hill & Lilly 1991; Allington-Smith et al. 1993; Zirbel 1997). The $z \sim 1$ 3CR sources in particular lie in regions typically consistent with Abell class 0–1 clusters (Best 2000). If the density of the IGM surrounding a radio source is correlated with the richness of the local galaxy environment, this has implications for the other observed properties of the $z \sim 1$ 3CR radio sources. Under the conditions of a higher density IGM, the radio source will be subject to a somewhat greater level of confinement, boosting its observed luminosity and potentially also restricting the rapidity of its growth (e.g. Kaiser et al. 1997; Kaiser & Alexander 1999). The extreme radio luminosity of the high-redshift 3CR sources could possibly be caused by a richer environment than average. Given the limited differences between the properties of the $z \sim 1$ 3CR and 6C host galaxies, it is worth hypothesizing that the factor of 6 difference in their radio luminosities may in part be due to environmental effects, in addition to other factors such as the fuelling rate of the AGN. Analysis of the environments of the 6C sources at $z \sim 1$ suggests that they lie in Abell class 0 environments (Roche, Eales & Hippelein 1998), somewhat less rich on average than those of the 3CR sources at the same redshift.

Other environmental factors may also be important. It is now becoming increasingly likely that galaxy mergers/interactions are responsible for the triggering of most (if not all) radio sources at some level. The levels of gas involved in such a scenario, and therefore the subsequent fuelling of the AGN, star formation in the host galaxy and the density of the disturbed IGM surrounding the radio source, may all be strongly dependent on the properties of the local environment and the nature of the galaxies involved. As was noted in the preceding section, the emission from several of the larger 6C and 3CR sources at $z \sim 1$ is particularly blue in colour, and comparable to that of smaller sources which display a more extreme alignment effect. It is noteworthy that many of these sources also either display signs of interactions, or that they have a larger than average number of companion objects at a close projected distance; this may very well be an example of a richer environment leading to the boosting of activity in and around the radio galaxy, as well as maintaining relatively high radio luminosities out to large radio sizes. Scattered emission, jet–cloud interactions and jet-induced star formation could all take place more readily for a radio source in rich surroundings, leading to a stronger alignment effect; this could help explain the differences in the luminosity of the aligned emission observed between the powerful 3CR sources at $z \sim 1$ and the less powerful 6C sources at the same redshift. These factors may also help explain why the alignment effect is so much less extreme at lower redshifts for the sources in both the 6C and 3CR samples: low-redshift radio sources are predominantly found in less rich environments, and the merger history of the galaxies in question is likely to have been substantially different to that of higher-redshift sources.

4.2.2 Stellar populations of the host galaxies, and deviations from passive evolution

The final factor which requires consideration is the nature of the host galaxy stellar populations. Although the radio source host galaxies appear to be well-behaved de Vaucouleurs ellipticals (Inskip et al.

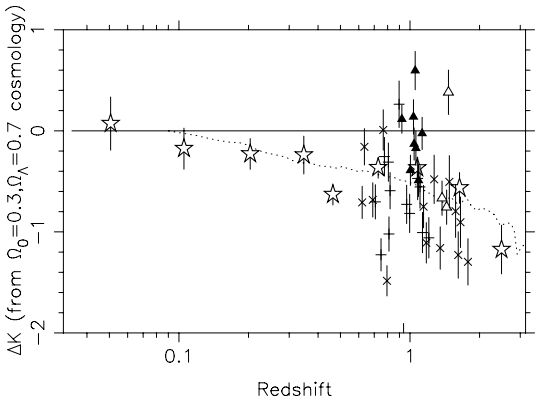

Figure 6. Deviations from the predictions of passive evolution models. The solid line represents the track for a passively evolving elliptical galaxy formed at $z = 10$ in a cosmological model with $\Omega_0 = 0.3$, $\Omega_\Lambda = 0.7$ and $H_0 = 65\,\mathrm{km\,s^{-1}\,Mpc^{-1}}$, and the dotted line represents the same model with $\Omega_0 = 1.0$, $\Omega_\Lambda = 0.0$ and $H_0 = 50\,\mathrm{km\,s^{-1}\,Mpc^{-1}}$. The models assume a fixed galaxy mass, normalized to fit the low-redshift data. The data points represent the magnitude difference between the passive evolution model and the observed data (such that negative values imply the galaxies are brighter than the model predictions): large stars represent the average K-band magnitudes for 57 6C galaxies with $z < 3.4$ and 72 3CR galaxies with $z < 1.8$, and the other symbols represent the data in the 6C and 3CR $z \sim 1$ subsamples as in Fig. 1. All data are evaluated in a 63.9-kpc aperture. There would be little change to this plot for a slightly later formation redshift of $z = 5$. The discrepancy between models and data would be substantially less for a formation redshift of $z = 3$, but other observational factors (e.g. red colours and the presence of radio sources at $z \gtrsim 5$) disfavour this scenario.

2005), with K-band emission dominated by an old passively evolving stellar population, this may not be a complete picture. There is increasing evidence that the host galaxy population for powerful radio galaxies evolves considerably with redshift. In the currently favoured cosmological model, the infrared magnitude–redshift relation for 6C and 3CR sources (Inskip et al. 2002a) suggests that at high redshifts, the most powerful 3CR radio galaxies are not only systematically more luminous in the K band than their less powerful 6C counterparts, but that both samples are more luminous than the predictions of passive evolution (assuming the same average mass at all redshifts). Fig. 6 displays this deviation from passive evolution for the complete 6C ER (Rawlings, Eales & Lacy 2001) and 3CR (Laing, Riley & Longair 1983) samples, plus the individual data for our $z \sim 1$ subsamples, clearly showing the increased luminosity for the higher-redshift and higher radio power systems. The most obvious mechanism by which the host galaxy can deviate from a simple passively evolving old stellar population is via an additional burst of star formation at some point in the galaxy's past, plausibly associated with a merger event which may also be responsible for triggering the production of a powerful radio source. It is certainly worthwhile investigating the effects of recent star formation in more detail, paying close attention to the constraints provided by the observational data. Our consideration of the influence of the host galaxy stellar populations on the observed galaxy colours is presented in the following section.

5 THE INFLUENCE OF THE HOST GALAXY STELLAR POPULATIONS

Variations in the stellar populations of the $z \sim 1$ 6C and 3CR host galaxies are likely to provide the best explanation for both their observed deviation from passive evolution models and their strikingly similar colours. A slightly later formation redshift for one of the samples is one option: this would lead to younger, more luminous, bluer host galaxies. The shapes of the SEDs for galaxies with ages between 2.5 and 5 Gyr (which encompasses the range of ages expected for a galaxy at $z \sim 1$, whose stellar populations formed at a redshift of 3–5) are very similar (e.g. Inskip et al. 2002a). F702W-K and F814W-K evolutionary tracks for galaxies formed at between redshifts of 3 and 10 are displayed in Fig. 1; tracks for the predicted $J - K$ colours are displayed in Fig. 3. At $z \sim 1$, the predicted $J - K$ colours for different star formation redshifts vary by less than $\sim$0.1 mag; changes in the observed F702W-K and F814W-K colours at $z \sim 1$ are not much greater, at $\lesssim$0.3 mag. Younger 6C host galaxies could therefore provide bluer F702W-K and F814W-K colours than would otherwise be expected; this bluening could balance the blue 3CR colours caused by the stronger alignment effect of the 3CR sources, leading to similar overall colours. It could similarly reduce any difference between the $J - K$ colours of the two samples. However, the K-band data require that of the two samples, the host galaxies of the more powerful 3CR sources should be the more luminous, which contradicts the possibility of younger 6C host galaxies. Secondly, if the 3CR sources are hosted by significantly younger galaxies, we would then need to explain how the 6C sources could match the bluer colours of the younger 3CR sources, unless the 3CR sources are also heavily reddened. Finally, there is no real physical justification for the age of the host galaxy having any impact on the power of a radio source produced at much later times.

The alternative option is a YSP accounting for only a small fraction of the total stellar mass of the host galaxy, formed at some point in its recent history. In addition to star formation associated with the passage of the expanding radio source (van Breugel et al. 1985; Best et al. 1997a), star formation associated with a galaxy merger and/or interaction is also a viable possibility, particularly since the triggering of the radio source activity may very well be linked with such processes (e.g. Johnston et al. 2005). There is increasing evidence that the host galaxies of distant radio sources include a contribution from a relatively young stellar population (e.g. Aretxaga et al. 2001), with an age of the order of that of the radio source. Whilst the presence of a YSP of such an age is entirely plausible, recent research (e.g. Tadhunter et al. 2002; Wills et al. 2002; Tadhunter et al. 2005) has identified the clear presence of older populations of young stars, with ages of between 0.1 and 2 Gyr. This scenario is in good agreement with recent results of the Sloan Digital Sky Survey (Kauffmann et al. 2003), which suggested that the host galaxies of the highest-luminosity AGN contain similarly young stellar populations. Although necessarily involving a greater proportion of the host galaxy stellar mass than a younger population of stars, such populations could easily account for an increased observed K-band luminosity without causing excessive boosting of the rest-frame UV flux.

We have used the GISSEL spectral synthesis models of Bruzual & Charlot (2003) to investigate the effects of a YSP on the host galaxy emission at different wavelengths. The formation of the youngest YSPs which we consider is assumed to be simultaneous with the triggering of the radio source itself, i.e. implying an age of $\lesssim 10^8$ yr, whilst we also consider older ages, up to a Gyr. Fig. 7 displays the predicted $J - K$, F814W-K and F702W-K colours for a $\sim$5-Gyr-old galaxy at $z = 1$, including a contribution from YSPs of varying ages. Also displayed are the predicted colours for a galaxy composed of a mixture of old stellar population and a reddenned 5×10^7-yr-old YSP. The resulting increase in the observed K-band emission for these models is displayed in Fig. 8. Fig. 9 displays the variations in

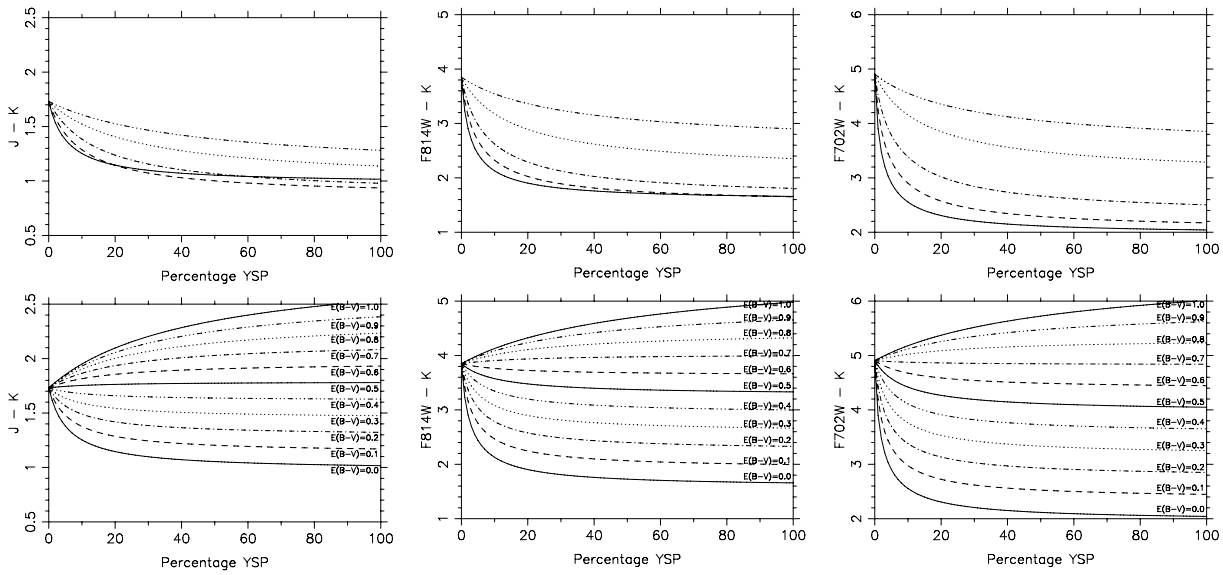

Figure 7. Plot displaying the predicted variations in galaxy colours at $z \sim 1$ given the inclusion of a YSP. The top row presents the predicted $J - K$ (left-hand panels), F814W-K (centred panels) and F702W-K (right-hand panels) colours as a function of percentage YSP, assuming a galaxy composed of old stellar population formed at $z = 5$, and a YSP with an age of either 5×10^7 yr (solid track), 1×10^8 yr (dashed track), 2×10^8 yr (dot–dashed track), 5×10^8 yr (dotted track) and 1×10^9 yr (double dot–dashed track). The lower row displays the same galaxy colours at $z \sim 1$, with the addition of a 5×10^7-yr-old YSP affected by varying levels of reddening [$E(B - V)$ ranging from 0.0 to 1.0].

F814W-K and F702W-K colours induced by the presence of these YSPs of different ages, given the requirement that the observed K-band emission is increased by a specified level (of between 0.3 and 1.0 mag).

Our observations (Fig. 1, which have F814W-K $\gtrsim$ 2–3 and F702W-K $\gtrsim$ 3–4) allow us to imply limits on the YSP mass fraction. A 5×10^7-yr YSP must account for <5 per cent of the total stellar mass of the galaxy if it is to lead to an increase in the observed K-band luminosity of <0.5 mag. The corresponding limit for a 10^8-yr-old YSP is $\lesssim$9 per cent of the galaxy stellar mass. Smaller bursts of star formation triggered by the expanding radio source would produce colours in good agreement with those observed for the aligned emission in these systems. These limits can be relaxed with the inclusion of reddening; with an $E(B - V)$ of 1.0, a 5×10^7-yr-old YSP accounting for 15 per cent of the total galaxy mass will not produce either excessively blue colours, or an excessively large increase in the observed K-band flux.

However, in order for a YSP to produce any difference between 3C and 6C colours, we would need to consider the radio power dependence of the properties of any YSP. If we assume that the rest-frame UV excess due to the alignment effect for the 6C sources is equal to or weaker than that of the 3CR sources, then the 6C host galaxies must be bluer on average than those of the 3CR sample, in order to obtain comparable colours for the two samples. Whilst this could be achieved with a stronger YSP contribution for the 6C sources than the 3CR sources, the luminosity differences between the samples rule this option out. The alternative is to include reddening of both the old and young stellar populations of the 3CR host galaxies; however, it is not clear that the levels of reddening should depend in any way on the radio power of the source in question.

The observed YSP ages are in many cases significantly older than the radio source itself, and it is therefore difficult to relate the properties of a YSP of such an age with the power of the radio source (although links could possibly be found by considering the exact details of any merger event associated with the formation of a YSP, and the much later triggering of the radio source/AGN activity; both factors may also be related to the host galaxy environment). This implies that it is unlikely that the presence of older YSPs can account for the observed differences between the 3CR and 6C host galaxies at $z \sim 1$. However, the presence of an 'old' YSP may explain why radio source host galaxies are bluer than expected given the predictions of passive evolution models. In order to increase the K-band emission by 0.5 mag (i.e. the observed difference between radio galaxies and passive evolution models at $z \sim 1$; Inskip et al. 2002a), a YSP $\gtrsim$ 0.5 Gyr in age and containing $\gtrsim$20 per cent of the host galaxy mass is required; this is in excellent agreement with the findings of Tadhunter et al. (2005).

6 CONCLUSIONS

The major results of our analysis of the $z \sim 1$ galaxy colours can be summarized as follows.

(i) The observed infrared colours of the 6C and 3CR sources are indistinguishable, and well explained by passively evolving galaxies up to redshifts of $\sim$1.3.

(ii) The galaxy colours begin to deviate from passive old stellar populations at higher redshifts ($z \gtrsim 1.3$), as increasing amounts of redshifted aligned emission lie in the wavelength range of the infrared filters.

(iii) The observed F702W-K and F814W-K colours become increasingly blue out to redshifts of $z \approx 1.1$, and then redden again at higher redshifts. This is linked to the fact that the excess rest-frame UV emission produced by the aligned structures becomes increasingly important between redshifts of 0.6 and 1, and that as redshift increases beyond that, the underlying old stellar population of elliptical galaxies can be expected to have increasingly red colours in these observed wavebands.

(iv) The observed F702W-K and F814W-K colours for both galaxy samples are also statistically indistinguishable, suggesting

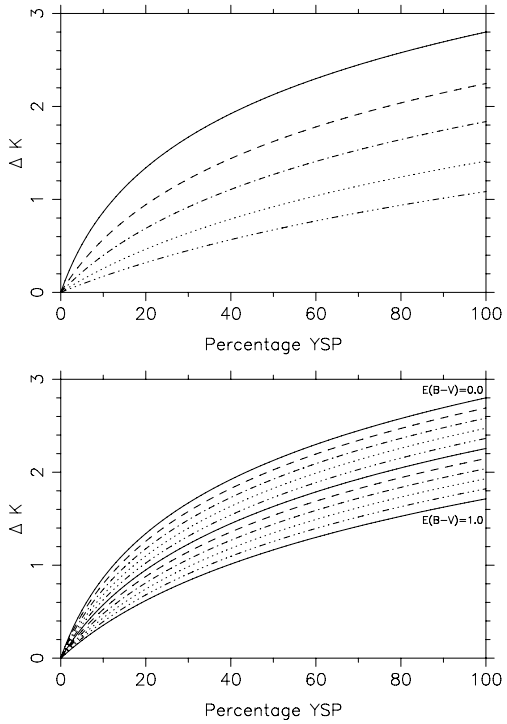

Figure 8. Plots displaying tracks for predicted variation in K-band magnitude produced by the addition of a YSP to a 5×10^9-yr-old stellar population (consistent with a $z \sim 1$ galaxy with a star formation redshift of $z \sim 5$). Top: Change in K-band magnitude with the addition of model YSP ages of 5×10^7 yr (solid track), 1×10^8 yr (dashed track), 2×10^8 yr (dot–dashed track), 5×10^8 yr (dotted track) and 1×10^9 yr (double dot–dashed track). Bottom: Change in K-band magnitude with the addition of a reddened 5×10^7-yr-old YSP, with $E(B-V)$ values ranging from 0.0 to 1.0.

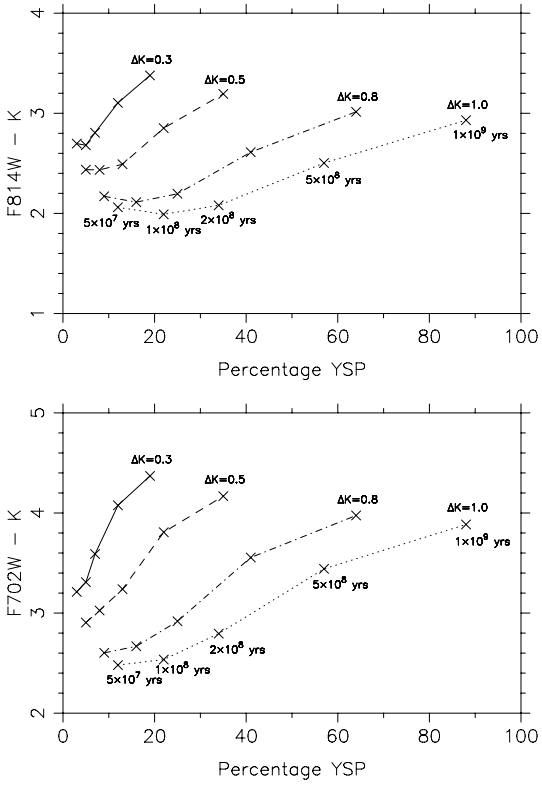

Figure 9. Plot displaying the tracks for predicted F814W-K (top) and F702W-K (bottom) colours, and the percentage contributions of YSPs which would be required in order to increase the K-band magnitude of the host galaxy by 0.3, 0.5, 0.8 or 1.0 mag. The models consider young stellar populations with ages of $5 \times 10^7, 1 \times 10^8, 2 \times 10^8, 5 \times 10^8$ and 1×10^9 yr, in conjunction with a 5×10^9-yr old stellar population (consistent with a $z \sim 1$ galaxy with a star formation redshift of $z \sim 5$).

that either the predominant alignment effect mechanisms do not scale strongly with radio power, or that some additional effect works to counterbalance this.

(v) Just as the most extreme rest-frame UV morphologies are generally associated with the smaller radio sources in the sample, these sources were also observed to display bluer colours due to the increased excess rest-frame UV emission observed on the *HST*/WFPC2 images. We see some signs that galaxy environment affects the strength of the observed alignment effect.

The interpretation of these results is not totally straightforward. Whilst the overall redshift evolution of the galaxy colours can be readily understood, the (lack of) variation in the observed optical–IR colours between the two $z \sim 1$ subsamples is less easily accounted for. The 3CR radio sources are around six times more powerful than those of the 6C subsample at $z \sim 1$, but the difference in mean K-band flux between the two data sets is much lower, at a factor of $\lesssim 2$. Given the fact that the emission produced by many alignment effect mechanisms should scale with radio power one might expect the more powerful sources to display bluer colours. Several mechanisms for producing the excess rest-frame UV-aligned emission will not necessarily produce more emission in the presence of a more luminous radio source. Star formation triggered by the expanding radio source through the surrounding IGM could potentially be more efficient for the 6C sources. The passage of a less powerful radio source may lead to lower levels of cloud shredding, and thus allow greater amounts of star formation. Additionally, the AGN of the more powerful 3CR galaxies are likely to heat and ionize the gas clouds to a greater extent, impeding the star formation rate within such clouds. However, observations of the mJy radio sources LBDS 53W091 and LBDS 53W069 at $z \sim 1.5$ (Spinrad et al. 1997; Dunlop 1999) would seem to contradict this hypothesis. These very low-power radio galaxies have very red stellar populations consistent with ages of over 3.5 Gyr. The observations of both galaxies are consistent with a de Vaucouleurs law luminosity profile, and neither displays any aligned emission. But, this may be a reflection of the radio properties of these sources (largest angular sizes are 4.2 and <5.1 arcsec, respectively). The disturbance to the IGM caused by such small, low-power radio galaxies may not be sufficient to trigger any extra star formation at all.

It should be noted that evidence for star formation is not restricted to sources displaying a strong alignment effect, and that a large variety of stellar populations are observed in different systems. UV *HST* observations of very low redshift 3CR sources (Allen et al. 2002) show that a high proportion of sources display some level of recent or ongoing star formation, without any need for a large-scale alignment effect. Very young (several Myr old) stellar populations accounting for $\lesssim 1$ per cent of the total stellar mass are observed in the host galaxies of the intermediate redshift compact radio sources PKS1345+12 (Rodriguez et al. private communication) and 9C1503+4528 (Inskip et al., in preparation), whilst a wider study of 2Jy and 3CR radio galaxies (Wills et al. 2002; Tadhunter

et al. 2005; Holt private communication) revealed evidence for older (0.05–2 Gyr), more massive (up to 50 per cent of the total stellar mass) stellar populations. Such varied stellar populations are likely to account for much of the scatter within different samples. However, this does not prevent us from drawing conclusions regarding the more general effects of properties such as radio power on the samples as a whole.

One important consideration is whether star formation induced by an expanding radio source may instead depend more strongly on the mass of available gas, rather than any other parameters. Scattering processes are also likely to depend on the available mass of gas and dust as well as on the power of the rest-frame UV emission from the AGN. If true, the fact that the 6C and 3CR host galaxies at $z \sim 1$ are of comparable size would be a point in favour of similar masses and hence observed colours. However, the total mass of cool clouds in the regions of the IGM surrounding the host galaxy may or may not scale with galaxy mass. If, for example, the radio source is triggered by a galaxy merger, the scattering processes may depend most strongly on the amount of dust and gas brought in by that merger. A further consideration is whether the 3CR sources lie in particularly rich environments, which may boost both their observed radio luminosity and also the availability of gas in the surrounding IGM.

Two main mechanisms are known/expected to vary with radio source size (and plausibly age). Emission-line flux scales strongly with radio source size as well as radio power, due to the increased importance of shock excitation in smaller, younger radio sources. Blue galaxy colours due to jet induced star formation should also weaken at larger radio sizes, due to the rapid aging of the recently formed YSP. Although radio power does not appear to strongly influence the observed galaxy colours, it is noticeable that the trends observed with radio source size in the case of the more powerful 3CR data are considerably weaker (or absent) at the lower powers of the $z \sim 1$ 6C sample, particularly after the removal of emission-line contamination. The lack of any clear-cut trend in these data does not rule out jet-induced star formation as an important mechanism for producing the alignment effect, but rather indicates that the high level of scatter, due to other processes and the influence of the local environment/IGM, has swamped any underlying evolution of the alignment effect with source age/size. Given the comparable colours between the samples and the distinct lack of discrete blue components at any great distance from the 6C host galaxies, it is certainly clear that the bulk of the excess rest-frame UV emission lies closer to the host galaxies (or indeed within them) in the case of the 6C sources.

Finally, it seems likely that the most important factor in explaining these data is not variations in the origin or nature of the rest-frame UV excess in each sample, but the longer wavelength emission of our *K*-band data. The *K*-band emission from the more powerful 3CR sources is increased over the levels expected from passive evolution scenarios, suggesting that the presence of a YSP (or at least one more youthful than the majority old stellar population) may be skewing the galaxy colours. The presence of either a reddened YSP of similar age to the radio source itself (i.e. $\gtrsim 10^7$ yr), or an older population of up to a Gyr or so in age, can account for the excess *K*-band emission from the more powerful sources without leading to substantially bluer emission from the host galaxy. However, given that the rest-frame UV excess must be balanced by any long-wavelength emission from an additional stellar population (in order that the lack of any colour difference between the samples is thereby maintained), it seems certain that reddening effects within the host galaxy are also an important factor.

ACKNOWLEDGMENTS

KJI acknowledges the support of a Lloyds Tercentenary Foundation Research Fellowship and a PPARC postdoctoral research fellowship. PNB is grateful for the generous support offered by a Royal Society Research Fellowship. The UKIRT is operated by the Joint Astronomy Centre on behalf of the UK Particle Physics and Astronomy Research Council. Some of the data reported here were obtained as part of the UKIRT Service Programme. Parts of this research are based on observations made with the NASA/ESA *HST*, obtained at the Space Telescope Science Institute, which is operated by the Association of Universities for Research in Astronomy, Inc., under NASA contract NAS 5-26555. These observations are associated with proposals #6684 and #8173.

REFERENCES

Allen M. G. et al., 2002, ApJS, 139, 411
Allington-Smith J. R., Ellis R., Zirbel E. L., Oemler A., 1993, ApJ, 404, 521
Aretxaga I., Terlevich E., Terlevich R. J., Cotter G., Díaz A. I., 2001, MNRAS, 325, 636
Begelman M. C., Cioffi D. F., 1989, ApJ, 345, L21
Best P. N., 1996, PhD thesis, Cavendish Laboratory, Cambridge University
Best P. N., 2000, MNRAS, 317, 720
Best P. N., Longair M. S., Röttgering H. J. A., 1996, MNRAS, 280, L9
Best P. N., Longair M. S., Röttgering H. J. A., 1997a, MNRAS, 286, 785
Best P. N., Longair M. S., Röttgering H. J. A., 1997b, MNRAS, 292, 758
Best P. N., Longair M. S., Röttgering H. J. A., 1998, MNRAS, 295, 549
Best P. N., Eales S. A., Longair M. S., Rawlings S., Röttgering H. J. A., 1999, MNRAS, 303, 616
Best P. N., Röttgering H. J. A., Longair M. S., 2000a, MNRAS, 311, 1
Best P. N., Röttgering H. J. A., Longair M. S., 2000b, MNRAS, 311, 23
Blundell K. M., Rawlings S., 2000, AJ, 119, 1111
Blundell K. M., Rawlings S., Willot C. J., 1999, ApJ, 117, 677
Bremer M. N., Fabian A. C., Crawford C. S., 1997, MNRAS, 284, 213
Bruzual G., Charlot S., 2003, MNRAS, 344, 1000
Chambers K. C., McCarthy P. J., 1990, ApJ, 354, L9
Chambers K. C., Miley G. K., van Breugel W. J. M., 1987, Nat, 329, 604
Cimatti A., di Serego Alighieri S., Fosbury R. A. E., Salvati M., Taylor D., 1993, MNRAS, 264, 421
Cotter G., 1998, in Bremer M. N., Jackson N., Perez-Fournon I., eds, Astrophysics and Space Science Library (ASSL) Series, 226, Observational Cosmology with the New Radio Surveys. Kluwer, Dordrecht, p. 233
Dickson R., Tadhunter C., Shaw M., Clark N., Morganti R., 1995, MNRAS, 273, L29
Dunlop J. S., 1999, in Röttgering H. J. A., Best P. N., Lehnert M. D., eds, The Most Distant Radio Galaxies. Royal Netherlands Academy of Arts and Sciences, Amsterdam, p. 71
Fanti C. et al., 2000, A&A, 358, 499
Fosbury R. A. E., Vernet J., Villar-Martín M., Cohen M. H., Ogle P. M., Tran H. D., Hook R. N., 1999, in Röttgering H. J. A., Best P. N., Lehnert M. D., eds, The Most Distant Radio Galaxies. Royal Netherlands Academy of Arts and Sciences, Amsterdam, p. 311
Hill G. J., Lilly S. J., 1991, ApJ, 367, 1
Icke V., 1999, in Röttgering H. J. A., Best P. N., Lehnert M. D., eds, The Most Distant Radio Galaxies. Royal Netherlands Academy of Arts and Sciences, Amsterdam, p. 217
Inskip K. J., Best P. N., Longair M. S., MacKay D. J. C., 2002a, MNRAS, 329, 277
Inskip K. J., Best P. N., Rawlings S., Longair M. S., Cotter G., Röttgering H. J. A., Eales S. A., 2002b, MNRAS, 337, 1381
Inskip K. J., Best P. N., Röttgering H. J. A., Rawlings S., Cotter G., Longair M. S., 2002c, MNRAS, 337, 1407
Inskip K. J., Best P. N., Longair M. S., Rawlings S., Röttgering H. J. A., Eales S., 2003, MNRAS, 345, 1365
Inskip K. J., Best P. N., Longair M. S., 2004, New Astron. Rev., 47, 255

Inskip K. J., Best P. N., Longair M. S., Röttgering H. J. A., 2005, MNRAS, 359, 1393
Jarvis M. J. et al., 2001, MNRAS, 326, 1563
Johnston H. M., Hunstead R. W., Cotter G., Sadler E. M., 2005, MNRAS, 356, 515
Kaiser C. R., Alexander P., 1999, in Giuricin G., Mezetti M., Salucci P., eds, ASP Conf. Ser., Vol. 176, Observational Cosmology: The Development of Galaxy Systems. Astron. Soc. Pac., San Francisco
Kaiser C. R., Dennett-Thorpe J., Alexander P., 1997, MNRAS, 292, 723
Kauffmann G. et al., 2003, MNRAS, 346, 1055
Klein R. I., McKee C. F., Colella P., 1994, ApJ, 420, 213
Kormendy J., Richstone D., 1995, ARA&A, 33, 581
Lacy M., Ridgway S. E., Wold M., Lilje P. B., Rawlings S., 1999, MNRAS, 307, 420
Laing R. A., Riley J. M., Longair M. S., 1983, MNRAS, 204, 151
Lara L., Giovannini G., Cotton W. D., Feretti L., Marcaide J. M., Márquez I., Venturi T., 2004, A&A, 421, 899
Mack K.-H., Klein U., O'Dea C. P., Willis A. G., Saripalli L., 1998, A&A, 329, 431
McCarthy P. J., 1993, ARA&A, 31, 639
McCarthy P. J., Spinrad H., van Breugel W. J. M., 1995, ApJS, 99, 27
McCarthy P. J., van Breugel W. J. M., Spinrad H., Djorgovski S., 1987, ApJ, 321, L29
McLure R. J., Willott C. J., Jarvis M. J., Rawlings S., Hill G. J., Mitchell E., Dunlop J. S., Wold M., 2004, MNRAS, 351, 347
Mellema G., Kurk J. D., Röttgering H. J. A., 2002, A&A, 395, L13
Neeser M. J., Eales S. A., Law-Green J. D., Leahy J. P., Rawlings S., 1995, ApJ, 451, 76
O'Dea C. P., 1998, PASP, 110, 493
Ojha R., Fey A. L., Johnston K. J., Jauncey D. L., Tzioumis A. K., Reynolds J. E., 2004, AJ, 127, 1977
Osterbrock D. E., 1989, Astrophysics of Gaseous Nebulae and Active Galactic Nuclei. University Science Books, Mill Valley
Pentericci L., McCarthy P. J., Röttgering H. J. A., Miley G. K., van Breugel W. J. M., Fosbury R., 2001, ApJS, 135, 63
Poludnenko A. Y., Frank A., Blackman E., 2002, ApJ, 576, 832
Rawlings S., Saunders R., 1991, Nat, 349, 138
Rawlings S., Eales S., Lacy M., 2001, MNRAS, 322, 523
Rees M. J., 1989, MNRAS, 239, 1P
Rigler M. A., Lilly S. J., Stockton A., Hammer F., Le Fèvre, 1992, ApJ, 385, 61
Roche N., Eales S. A., 2000, MNRAS, 317, 120
Roche N., Eales S. A., Hippelein H., 1998, MNRAS, 295, 946
Simpson C., Rawlings S., 2002, MNRAS, 334, 511
Smith E. P., Heckman T. M., 1989, ApJ, 341, 658
Solórzano-Iñarrea C., Tadhunter C. N., Axon D. J., 2001, MNRAS, 323, 965
Spinrad H., Dey H., Stern D., Dunlop J., Peacock J., Jiminez R., Windhorst R., 1997, ApJ, 484, 581
Tadhunter C. N., Scarrott S. M., Draper P., Rolph C., 1992, MNRAS, 256, 53
Tadhunter C. N., Dickson R., Morganti R., Robinson T. G., Wills K., Villar-Martin M., Hughes M., 2002, MNRAS, 330, 977
Tadhunter C. N., Robinson T. G., González Delgado R. M., Wills K., Morganti R., 2005, MNRAS, 356, 480
Tran H. D., Cohen M. H., Ogle P. M., Goodrich R. W., di Serego Alighieri S., 1998, ApJ, 500, 660
Tzioumis A. et al., 2002, A&A, 392, 841
van Breugel W. J. M., Dey A., 1993, ApJ, 414, 563
van Breugel W. J. M., Filippenko A. V., Heckman T., Miley G., 1985, ApJ, 293, 83
van Breugel W. J. M., Stanford S. A., Spinrad H., Stern D., Graham J. A., 1998, ApJ, 502, 614
Willott C. J., Rawlings S., Blundell K. M., Lacy M., 1999, MNRAS, 309, 1017
Wills K. A. Tadhunter C. N., Robinson T. G., Morganti R., 2002, 333, 211
Zirbel E. L., 1997, ApJ, 476, 489
Zirm A. W., Dickinson M., Dey A., 2003, ApJ, 585, 90

This paper has been typeset from a TEX/LATEX file prepared by the author.